

Algebraic Robustness Verification of Neural Networks

Yulia Alexandr^{1,†}

UCLA

yulia@math.ucla.edu

Hao Duan^{2,†}

UCLA

hduan7@ucla.edu

Guido Montúfar^{1,2,3}

UCLA & MPI MiS

montufar@math.ucla.edu

Abstract

We formulate formal robustness verification of neural networks as an algebraic optimization problem. We leverage the Euclidean Distance (ED) degree, which is the generic number of complex critical points of the distance minimization problem to a classifier’s decision boundary, as an architecture-dependent measure of the intrinsic complexity of robustness verification. To make this notion operational, we define the associated ED discriminant, which characterizes input points at which the number of real critical points changes, distinguishing test instances that are easier or harder to verify. We provide an explicit algorithm for computing this discriminant. We further introduce the parameter discriminant of a neural network, identifying parameters where the ED degree drops and the decision boundary exhibits reduced algebraic complexity. We derive closed-form expressions for the ED degree for several classes of neural architectures, as well as formulas for the expected number of real critical points in the infinite-width limit. Finally, we present an exact robustness certification algorithm based on numerical homotopy continuation, establishing a concrete link between metric algebraic geometry and neural network verification.

Keywords: ED degree, ED discriminant, Kac-Rice formula, parameter discriminant, robustness verification, decision boundary

1 Introduction

The deployment of neural networks in safety-critical settings has led to a growing demand for formal robustness guarantees, ensuring that small perturbations of the input do not lead to incorrect or unsafe predictions. Robustness verification, certifying that a classifier’s output remains invariant over a specified neighborhood of an input, is therefore a central problem in modern machine learning.

A wide range of verification methods have been proposed, including convex relaxations (Salman et al., 2019), mixed-integer programming (Tjeng et al., 2019), satisfiability modulo theories (Katz et al., 2017), and abstract interpretation (Gehr et al., 2018). While these approaches have achieved success in various settings (Weng et al., 2018; Zhang et al., 2018; Botoeva et al., 2020; Brix et al., 2023), they all face a tradeoff between exactness and scalability: exact methods often suffer from exponential complexity or strong dependence on specific architectures (Meng et al., 2022; Liu et al., 2024; Froese et al., 2025), whereas relaxed methods can achieve fast computation, but they may be loose (Singh et al., 2018; Wong and Kolter, 2018; Salman et al., 2019) and incapable to verify difficult instances. There is limited theoretical understanding of how the intrinsic structure of a neural network governs the complexity of robustness verification (Ferlez and Shoukry, 2021; König et al., 2024).

We propose an algebraic framework for robustness verification, treating neural networks and their decision boundaries as algebraic objects. For polynomial classifiers and, more generally, decision boundaries that are algebraic or semi-algebraic, robustness verification can be formulated as an algebraic distance minimization

[†] Equal contribution.

¹ Department of Mathematics, University of California, Los Angeles, CA 90095, USA

² Department of Statistics & Data Science, University of California, Los Angeles, CA 90095, USA

³ Max Planck Institute for Mathematics in the Sciences, 04103 Leipzig, Germany

problem (see Figure 1). In this case, the decision boundary, which is a set of input points satisfying an equation of the form $f_i(\mathbf{x}) - f_j(\mathbf{x}) = 0$, forms an algebraic variety. Robustness verification amounts to certifying that the distance from a given test point ξ to the decision boundary is bounded below by some ϵ . This perspective naturally connects robustness verification to tools from metric algebraic geometry, where the complexity of distance optimization is captured by algebraic invariants of the underlying variety.

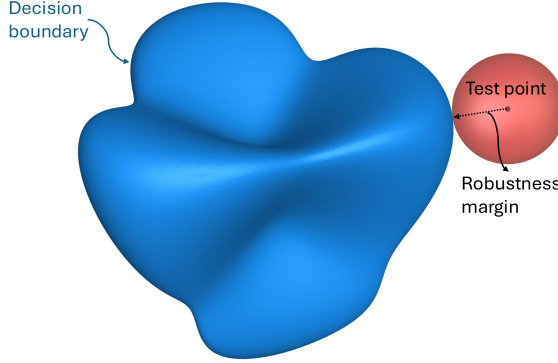


Figure 1: The blue hypersurface shows the decision boundary of a polynomial neural network. The black dot is a test input; we compute its projection onto this decision boundary to obtain the robustness margin.

Our central complexity measure is the Euclidean Distance (ED) degree, a fundamental invariant from algebraic geometry, defined as the generic number of complex critical points of the distance function to the decision boundary (Draisma et al., 2016; Maxim et al., 2020; Breiding et al., 2024; Lai et al., 2025). In the context of robustness verification, the ED degree provides an architecture-dependent notion of verification complexity, independent of optimization heuristics. We leverage this notion by introducing two discriminants. First, the *ED discriminant* characterizes input points at which the number of *real* critical points changes, thereby identifying test instances that are easier or harder to certify. We provide explicit algorithms for its computation. Second, the *parameter discriminant* identifies network parameters for which the ED degree drops, indicating reduced algebraic complexity of the decision boundary. We derive closed formulas for the ED degree for several classes of network architectures, as well as for the expected number of real critical points in the infinite-width limit. Finally, we present an exact robustness certification algorithm based on numerical homotopy continuation, yielding provably correct certificates whenever the algebraic problem can be solved.

1.1 Contributions

Our main contributions are summarized as follows:

- In Section 2, we formulate robustness verification as a metric projection problem onto algebraic varieties, providing an exact KKT-characterization and a relaxation.
- In Section 3, we propose the ED degree as a notion of verification complexity and outline its computation (Alg. 1).
- In Section 3.1, we derive closed-form expressions for the ED degree of decision boundaries under generic parameters for wide and bottleneck architectures (Prop. 3.8 and Prop. 3.6), and give numerical results for intermediate regimes.
- In Section 3.2, we derive a general formula for the expected number of real critical points (Prop. 3.10), and a result for Neural Network Gaussian Processes (NNGP) (Cor. 3.11).
- In Section 4.1, we define the ED discriminant, which classifies test instances by the complexity of the verification task. We provide a symbolic algorithm for its computation (Alg. 2), along with examples.
- In Section 4.2, we introduce the parameter discriminant, which classifies the parameters of a neural network by the verification complexity. We establish a complete characterization for quadric boundaries (Thm. 4.6) and derive the parameter discriminant as a stratified hypersurface.

An implementation of our algorithms is provided at: <https://github.com/edwardduanhao/AlgebraicVerification>.

1.2 Related Works

Neural network verification Formal verification of neural networks has been extensively studied using satisfiability modulo theories, mixed-integer programming, and abstract interpretation (Katz et al., 2017; Tjeng et al., 2019; Anderson et al., 2020; Gehr et al., 2018). These approaches provide exact or conservative robustness guarantees for piecewise-linear networks, notably ReLU architectures, but typically face a tradeoff between scalability and precision (Meng et al., 2022; Liu et al., 2024; Froese et al., 2025). While highly effective in practice, existing methods largely treat robustness as an algorithmic problem and offer limited insight into how architectural or geometric properties of a network govern the intrinsic complexity of verification.

Distance-based robustness Robustness verification can be formulated as the problem of computing the minimum distance from an input to the classifier’s decision boundary. This viewpoint underlies many adversarial robustness and certification methods based on local optimization (Szegedy et al., 2014; Carlini and Wagner, 2017) or convex relaxations (Wong and Kolter, 2018; Salman et al., 2019). Prior work focuses on computing or bounding adversarial perturbations (Hein and Andriushchenko, 2017; Raghunathan et al., 2018), but does not characterize the global structure or number of critical points of the optimization problem.

Algebraic perspectives on neural networks A growing body of work applies tools from algebraic geometry, tropical geometry, and related areas to the study of neural networks, addressing questions of expressivity (Kileel et al., 2019; Brandenburg et al., 2024; Kubjas et al., 2024; Alexandr and Montúfar, 2025), identifiability (Allman et al., 2009; Henry et al., 2025; Usevich et al., 2025), optimization landscapes (Venturi et al., 2019; Kohn et al., 2022). These works model neural networks as polynomial or piecewise-polynomial maps and analyze the resulting algebraic varieties or stratified spaces. In contrast, our focus is on formal robustness verification, rather than representation or training dynamics.

We connect these lines of research by introducing algebraic complexity measures based on the Euclidean Distance degree and associated discriminants for robustness verification. Our framework treats verification difficulty as an intrinsic function of architecture and parameters, and yields exact algorithms grounded in metric algebraic geometry.

2 Verification as an Algebraic Problem

Notation We use $[n]$ to denote the index set $\{1, 2, \dots, n\}$. For a given $\mathbf{u} = (u_1, \dots, u_n)^\top \in \mathbb{R}^n$ and any $\mathbf{x} = (x_1, \dots, x_n)^\top \in \mathbb{R}^n$, we define the squared Euclidean distance

$$d_{\mathbf{u}}(\mathbf{x}) := \sum_{i=1}^n (x_i - u_i)^2.$$

For a center $\mathbf{x}_0 \in \mathbb{R}^n$ and radius $r > 0$, we define the open Euclidean ball as

$$\mathbb{B}(\mathbf{x}_0, r) := \{\mathbf{x} \in \mathbb{R}^n \mid d_{\mathbf{x}_0}(\mathbf{x}) < r^2\}.$$

2.1 Robustness Verification via Metric Projection

Let $f_{\boldsymbol{\theta}} : \mathbb{R}^n \rightarrow \mathbb{R}^k$ be a parametric model for k -class classification, with parameters $\boldsymbol{\theta} \in \mathbb{R}^p$. For any input $\mathbf{x} \in \mathbb{R}^n$, the model outputs a score vector $[f_{\boldsymbol{\theta},1}(\mathbf{x}), \dots, f_{\boldsymbol{\theta},k}(\mathbf{x})]$, and predicts $\arg \max_i f_{\boldsymbol{\theta},i}(\mathbf{x})$.

The standard formulation of robustness verification (Wong and Kolter, 2018) is as follows: given a test point $\boldsymbol{\xi} \in \mathbb{R}^n$ assigned to class c , we seek to certify that the predicted class remains invariant under all ℓ_2 perturbations of radius ϵ . Formally, the condition we want to verify is

$$\arg \max_{i \in [k]} f_{\boldsymbol{\theta},i}(\mathbf{x}) = c, \quad \forall \mathbf{x} \in \mathbb{B}(\boldsymbol{\xi}, \epsilon).$$

This condition can be reformulated as an optimization problem. For a fixed c , we define the worst-case margin as

$$\delta(\epsilon) := \min_{c' \neq c} \inf_{\mathbf{x} \in \mathbb{B}(\xi, \epsilon)} \{f_{\theta, c}(\mathbf{x}) - f_{\theta, c'}(\mathbf{x})\}.$$

If $\delta(\epsilon) \geq 0$, then the score of class c exceeds all others in $\mathbb{B}(\xi, \epsilon)$, thereby certifying robustness at ξ .

Geometric interpretation We interpret robustness verification as computing a metric projection of the test point onto the classifier's decision boundary. Define the *active decision boundary* between classes c and c' as

$$\mathcal{B}_{c, c'}^{\theta} := \{\mathbf{x} \in \mathbb{R}^n : f_{\theta, c}(\mathbf{x}) = f_{\theta, c'}(\mathbf{x}) = \max_{i \in [k]} f_{\theta, i}(\mathbf{x})\},$$

and denote the zero level set of logit difference as

$$\mathcal{V}_{c, c'}^{\theta} := \{\mathbf{x} \in \mathbb{R}^n : f_{\theta, c}(\mathbf{x}) - f_{\theta, c'}(\mathbf{x}) = 0\}.$$

Note that $\mathcal{B}_{c, c'}^{\theta} \subseteq \mathcal{V}_{c, c'}^{\theta}$, since the decision boundary requires extra constraints $f_{\theta, i}(\mathbf{x}) - f_{\theta, c}(\mathbf{x}) \leq 0$ for all $i \neq c, c'$.

We quantify the robustness margin as the minimum distance from the test point ξ to the active decision boundary,

$$\gamma := \min_{c' \neq c} \inf_{\mathbf{x} \in \mathcal{B}_{c, c'}^{\theta}} \sqrt{d_{\xi}(\mathbf{x})}. \quad (1)$$

The condition $\gamma \geq \epsilon$ implies that the ball $\mathbb{B}(\xi, \epsilon)$ does not intersect any active decision boundary, i.e.,

$$\mathbb{B}(\xi, \epsilon) \cap \bigcup_{c' \neq c} \mathcal{B}_{c, c'}^{\theta} = \emptyset.$$

Equivalently, for every $\mathbf{x} \in \mathbb{B}(\xi, \epsilon)$ and every $c' \neq c$, we have $f_{\theta, c}(\mathbf{x}) \geq f_{\theta, c'}(\mathbf{x})$, so the pairwise margins remain nonnegative everywhere in the ball, and $\delta(\epsilon) \geq 0$. By continuity of the logits, the predicted class then remains invariant within $\mathbb{B}(\xi, \epsilon)$, thereby certifying robustness at ξ .

2.2 Algebraic Optimization Formulation

We focus on the case where the classifier f_{θ} is *algebraic*, meaning each component $f_{\theta, i}$ is a polynomial of the input \mathbf{x} . In this setting, $\mathcal{V}_{c, c'}^{\theta}$ is a *real algebraic variety*, as it is the set of zeros of the polynomial $f_{\theta, c}(\mathbf{x}) - f_{\theta, c'}(\mathbf{x})$. Imposing the additional inequality constraints $f_{\theta, i}(\mathbf{x}) - f_{\theta, c}(\mathbf{x}) \leq 0$ for all $i \neq c, c'$ restricts this to a *semialgebraic* set $\mathcal{B}_{c, c'}^{\theta}$.

To compute the robustness margin γ , we formulate a constrained metric projection problem for each $c' \neq c$:

$$\begin{aligned} & \text{minimize} && d_{\xi}(\mathbf{x}) \\ & \text{subject to} && f_{\theta, c'}(\mathbf{x}) - f_{\theta, c}(\mathbf{x}) = 0, \\ & && f_{\theta, i}(\mathbf{x}) - f_{\theta, c}(\mathbf{x}) \leq 0, \quad \forall i \neq c, c'. \end{aligned} \quad (2)$$

This computes the projection of the test point ξ onto the active decision boundary between classes c and c' .

KKT conditions To characterize candidate solutions of Problem 2, we introduce the Lagrangian

$$\begin{aligned} \mathcal{L}(\mathbf{x}, \lambda, \mu) := & \frac{1}{2} d_{\xi}(\mathbf{x}) + \lambda(f_{\theta, c'}(\mathbf{x}) - f_{\theta, c}(\mathbf{x})) \\ & + \sum_{i \neq c, c'} \mu_i(f_{\theta, i}(\mathbf{x}) - f_{\theta, c}(\mathbf{x})), \end{aligned}$$

where λ and $\mu = (\mu_i)_{i \neq c, c'}$ are the KKT multipliers corresponding to the equality and inequality constraints.

By the KKT conditions (Karush, 1939; Kuhn and Tucker, 2014), any local optimum $(\mathbf{x}^*, \lambda^*, \mu^*)$ satisfies

$$\begin{cases} \nabla_{\mathbf{x}} \mathcal{L}(\mathbf{x}^*, \lambda^*, \mu^*) = 0, \\ f_{\theta, c'}(\mathbf{x}^*) - f_{\theta, c}(\mathbf{x}^*) = 0, \\ \mu_i^*(f_{\theta, i}(\mathbf{x}^*) - f_{\theta, c}(\mathbf{x}^*)) = 0, \quad \forall i \neq c, c', \\ f_{\theta, i}(\mathbf{x}^*) - f_{\theta, c}(\mathbf{x}^*) \leq 0, \quad \forall i \neq c, c', \\ \mu_i^* \geq 0, \quad \forall i \neq c, c'. \end{cases} \quad (3)$$

The first three conditions in (3) form a square system of $n + k - 1$ polynomial equations in $n + k - 1$ unknowns, while the remaining conditions encode feasibility constraints.

Since all equations are polynomial, the KKT system can be solved using tools from numerical algebraic geometry. We consider specifically *homotopy continuation* because it is a complete numerical method guaranteed to find all isolated complex solutions (Li, 1997; Sommese et al., 2001; Sommese and Wampler, 2005; Sommese et al., 2005; Duff et al., 2018). This computes all complex solutions to the stationarity, complementary slackness, and equality constraints. Subsequently, one retains the minimal real solution satisfying the remaining feasibility conditions. Figure 2 illustrates the concept, with details in Section A.

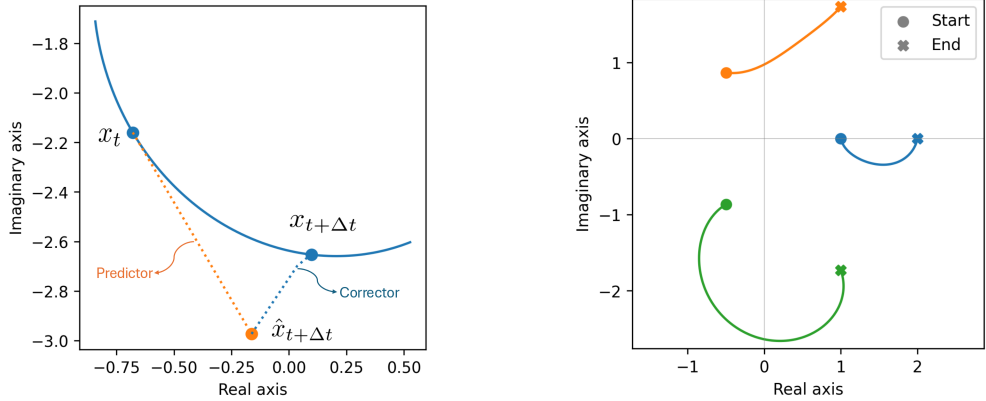


Figure 2: Left: An iteration of homotopy continuation, moving from x_t to $x_{t+\Delta t}$ via a tangent predictor (orange) and a Newton corrector (blue). Right: Homotopy paths tracking the roots of $x^3 - 4x^2 + 8x - 8 = 0$ (with $x_{1,2} = 1 \pm \sqrt{3}i$ and $x_3 = 2$) from the start system $x^3 - 1 = 0$ (with $x_{1,2} = -\frac{1}{2} \pm \frac{\sqrt{3}}{2}i$ and $x_3 = 1$).

Solving the full KKT system can be of interest in some cases, but is computationally prohibitive in practice. The Bézout upper bound on the number of complex solutions (Bézout, 1779) grows exponentially in the number of variables.

Relaxation of inequality constraints To mitigate this complexity, we consider a relaxation that removes the inequality constraints, resulting in a projection problem onto $\mathcal{V}_{c,c'}^\theta$ instead of $\mathcal{B}_{c,c'}^\theta$. Define the relaxed robustness margin

$$\tilde{\gamma} := \min_{c' \neq c} \inf_{\mathbf{x} \in \mathcal{V}_{c,c'}^\theta} \sqrt{d_\xi(\mathbf{x})}. \quad (4)$$

This relaxation is exact under mild conditions:

Proposition 2.1. *Let $f_\theta : \mathbb{R}^n \rightarrow \mathbb{R}^k$ be a continuous classifier, and let $\hat{c}(\mathbf{x}) := \arg \max_{i \in [k]} f_{\theta,i}(\mathbf{x})$ denote the predicted class. Fix a test point $\xi \in \mathbb{R}^n$ and write $c := \hat{c}(\xi)$. Assume that the prediction at ξ is unique, i.e.,*

$$f_{\theta,c}(\xi) > f_{\theta,c'}(\xi) \quad \text{for all } c' \neq c.$$

Then, for γ and $\tilde{\gamma}$ defined in (1) and (4), we have $\gamma = \tilde{\gamma}$.

The proof is provided in Section B.1. As a consequence, we may consider the relaxed optimization problem

$$\begin{aligned} & \text{minimize} && d_\xi(\mathbf{x}) \\ & \text{subject to} && f_{\theta,c'}(\mathbf{x}) - f_{\theta,c}(\mathbf{x}) = 0. \end{aligned} \quad (5)$$

The corresponding Lagrangian is

$$\mathcal{L}(\mathbf{x}, \lambda) = \frac{1}{2} d_\xi(\mathbf{x}) + \lambda (f_{\theta,c'}(\mathbf{x}) - f_{\theta,c}(\mathbf{x})),$$

and the KKT conditions reduce to

$$\begin{aligned} \mathbf{x}^* - \xi + \lambda^* (\nabla f_{\theta,c'}(\mathbf{x}^*) - \nabla f_{\theta,c}(\mathbf{x}^*)) &= 0, \\ f_{\theta,c'}(\mathbf{x}^*) - f_{\theta,c}(\mathbf{x}^*) &= 0. \end{aligned} \quad (6)$$

Algorithm 1 Symbolic computation of the ED degree

Require: Network parameters θ , classes (c, c')

Ensure: ED degree of $\mathcal{V}_{c,c'}^\theta$

- 1: Sample a generic point $\mathbf{u} = (u_1, \dots, u_n) \in \mathbb{R}^n$.
- 2: Form the augmented Jacobian

$$AJ_{c,c'}^\theta = \begin{bmatrix} \mathbf{u} - \mathbf{x} \\ \nabla_{\mathbf{x}}(f_{\theta,c}(\mathbf{x}) - f_{\theta,c'}(\mathbf{x})) \end{bmatrix}.$$

- 3: Define the ideal

$$J_{c,c'}^\theta = I_{c,c'}^\theta + \langle \text{all 2-minors of } AJ_{c,c'}^\theta \rangle.$$

- 4: Saturate to remove the singular locus:

$$C_{c,c'}^\theta = (J_{c,c'}^\theta : \langle \nabla_{\mathbf{x}}(f_{\theta,c} - f_{\theta,c'}) \rangle^\infty).$$

- 5: **return** $\deg(C_{c,c'}^\theta)$.

These yield a square system of $n+1$ equations in $n+1$ unknowns, instead of $n+k-1$, resulting in substantial computational savings when the number of classes k is large. We provide an implementation in Section C.¹

3 ED Degree of a Decision Boundary

We analyze the complexity of the metric projection problem onto the decision boundary of a classifier using the *Euclidean Distance (ED) degree* from algebraic geometry.

Definition 3.1 (Euclidean Distance Degree). Let $\mathcal{V} \subseteq \mathbb{C}^n$ be a complex algebraic variety², and let

$$\mathcal{V}_{\text{reg}} := \mathcal{V} \setminus \mathcal{V}_{\text{sing}} = \{\mathbf{x} \in \mathcal{V} \mid \dim T_{\mathbf{x}} \mathcal{V} = \dim \mathcal{V}\}$$

denote its smooth locus. The *Euclidean Distance (ED) degree* of \mathcal{V} is the number of complex critical points of the squared Euclidean distance function $d_{\mathbf{u}}(\mathbf{x})$ with respect to a generic³ data point $\mathbf{u} \in \mathbb{R}^n$ restricted to \mathcal{V}_{reg} :

$$\text{EDdegree}(\mathcal{V}) := \#\{\mathbf{x} \in \mathcal{V}_{\text{reg}} \mid \mathbf{x} - \mathbf{u} \perp T_{\mathbf{x}} \mathcal{V}\},$$

where $T_{\mathbf{x}} \mathcal{V}$ denotes the tangent space of \mathcal{V} at \mathbf{x} and the orthogonality is with respect to the standard dot product.

In Problem 5, we minimize the distance from ξ to $\mathcal{V}_{c,c'}^\theta$. Let $I_{c,c'}^\theta = \langle f_{\theta,c}(\mathbf{x}) - f_{\theta,c'}(\mathbf{x}) \rangle$ denote the ideal generated by the logit difference for fixed θ . Note the ED degree is defined with respect to \mathbb{C} , which ensures the count of critical points is a generic invariant. We treat $\mathcal{V}_{c,c'}^\theta \subseteq \mathbb{C}^n$ as a complex algebraic variety by taking the Zariski closure.

The ED degree of $\mathcal{V}_{c,c'}^\theta$ is as an upper bound on the optimization complexity: for our data point ξ , the number of complex critical points is bounded above by $\text{EDdegree}(\mathcal{V}_{c,c'}^\theta)$, with equality holding when ξ is generic.

For fixed θ , the variety $\mathcal{V}_{c,c'}^\theta$ is a hypersurface, since its ideal is generated by a single polynomial. Its ED degree is computed via Algorithm 1, where the resulting ideal $C_{c,c'}^\theta$ is zero-dimensional (Draisma et al., 2016, Lemma 2.1), and hence has finitely many solutions. Its degree equals the ED degree of the decision boundary.

In the remainder of this section, we address the questions:

- (i) For a given architecture and *generic* parameters θ , what is the ED degree of the decision boundary $\mathcal{V}_{c,c'}^\theta$?
- (ii) What is the number of *real* critical points of the Euclidean distance minimization problem?

¹Our implementation is available at: <https://github.com/edwardduanhao/AlgebraicVerification>

²For a real variety $\mathcal{V}_{\mathbb{R}} \subseteq \mathbb{R}^n$, we consider its complexification $\mathcal{V} \subseteq \mathbb{C}^n$. The number of real critical points depends on the data \mathbf{u} , but the number of complex critical points is generically constant.

³In this context, a point is *generic* if it lies in a dense open Zariski subset of the parameter space. Specifically, it does not lie on the ED discriminant locus defined in Section 4.1.

3.1 ED Degree for Generic Parameters

In this subsection, we study the ED degree of the decision boundary for a parameter θ that is fixed to be generic. This reflects the typical complexity of the problem, noting that the non-generic parameters form a thin set of measure zero. Denote the polynomial of the boundary as $B_\theta(\mathbf{x}) = f_{\theta,c}(\mathbf{x}) - f_{\theta,c'}(\mathbf{x})$, so $\mathcal{V}_{c,c'}^\theta = \{\mathbf{x} \in \mathbb{R}^n \mid B_\theta(\mathbf{x}) = 0\}$. For shallow networks, we obtain the following result.

Proposition 3.2. *Consider a neural network with architecture (n, h, k) and a degree- d polynomial activation function. Assume the parameters θ are generic. The ED degree of the decision boundary $\mathcal{V}_{c,c'}^\theta$ is given by*

$$\text{EDdegree}(\mathcal{V}_{c,c'}^\theta) = d \sum_{i=0}^{m-1} (d-1)^i, \text{ where } m = \min\{n, h\}.$$

This result reveals that the algebraic complexity is governed by the layer bottleneck $m = \min\{n, h\}$, implying that the difficulty of exact verification grows exponentially with the width of the network even when the other dimension is fixed.

Corollary 3.3. *In the case of a quadratic activation $d = 2$, the summation simplifies to m , yielding an ED degree of $2m$.*

Example 3.4. For $d = 3$ and generic parameters, Proposition 3.2 yields the following values:

- Architecture $(3, 2, 2)$: $m = 2$, ED degree 9.
- Architecture $(3, 3, 2)$: $m = 3$, ED degree 21.
- Architecture $(4, 4, 2)$: $m = 4$, ED degree 45.

Remark 3.5 (Deep architectures). For the architecture (n, h_1, \dots, h_s, k) , the polynomial $B_\theta(\mathbf{x})$ has degree $D = d^s$. Unlike the shallow case, deep networks define nested functional compositions. This rigid algebraic structure often leads to *reducible* varieties rather than generic hypersurfaces. Consequently, substituting the total degree D into the generic formula of Proposition 3.2 yields only a theoretical upper bound, while the true ED degree may be strictly lower. This is seen in Proposition 3.6 and Table 1.

Computing the exact ED degree of deep networks is difficult and remains an open problem in general. However, for networks that constrict to width 1, the decision boundary factorizes into parallel copies of a shallow surface, allowing us to prove the following result.

Proposition 3.6. *Consider a deep neural network with architecture $(n, h_1, 1, \dots, 1, k)$ having s hidden layers and degree- d activation. Assume $h_1 \geq n$ and generic θ . Then*

$$\text{EDdegree}(\mathcal{V}_{c,c'}^\theta) = D \sum_{i=0}^{n-1} (d-1)^i,$$

where $D = d^s$ is the total composite degree of the network.

Example 3.7. The polynomial neural network with architecture $(2, 2, 1, 1, 2)$ and $d = 2$ has ED degree 16. This is four times smaller than the naive bound of 64 for a generic curve of degree 8, illustrating how the network's bottleneck structure significantly reduces algebraic complexity.

On the other hand, if the network maintains sufficient width, the decision boundary achieves maximal generic complexity.

Proposition 3.8. *Consider a deep neural network with architecture (n, h_1, \dots, h_s, k) . Assume degree- d activation, and $h_i \geq n$ for all $i \in [s]$. For generic parameters θ ,*

$$\text{ED degree}(\mathcal{V}_{c,c'}^\theta) = D \sum_{i=0}^{n-1} (D-1)^i,$$

where $D = d^s$ is the composite degree of the network.

For the intermediate layer width regime $(1 < h_i < n)$, we can compute specific cases numerically. We present examples in Table 1.

Table 1: Numerical ED degrees for deep architectures.

ARCHITECTURE ($n, [h_1, \dots, h_s], d$)	TOTAL DEGREE $D = d^s$	COMPUTED ED DEGREE
(3, [3, 2], 2)	4	36
(3, [3, 2], 3)	9	333
(3, [2, 3], 3)	9	81
(4, [4, 3], 2)	4	128
(4, [4, 2], 2)	4	64
(5, [5, 3], 2)	4	260
(3, [3, 2, 2], 2)	8	168
(3, [3, 3, 2], 2)	8	328

Remark 3.9. The results indicate that intermediate width architectures have ED degree between the theoretical bounds. Proposition 3.8 serves as a generic upper bound, and Proposition 3.6 serves as a constructive lower bound for fixed depth s , where width 1 minimizes the algebraic mixing of variables. For example, architecture (3, [3, 2], 2) yields ED degree 36, between the bounds 12 and 52, which is greater than the lower bound 12 and less than the generic upper bound 52. This suggests that the decision boundary lives on a sparse subvariety whose complexity depends on the specific rank constraints of the hidden layers.

Our framework allows us to distinguish between the geometric complexity of the boundary and the identifiability of the parameters. Let p be the number of parameters and N be the dimension of the space of degree- D polynomials. Let $\Phi : \mathbb{R}^p \rightarrow \mathbb{R}^N$ be the parameterization map sending weights to coefficients. The observed drop in ED degree is governed by the dimension of the image $\text{Im}(\Phi)$ relative to the ambient dimension N . For intermediate architectures, we typically have $\dim(\text{Im}(\Phi)) \ll N$. This strict inequality ensures that the decision boundary lies on a proper subvariety of the polynomial space, which explains the reduced algebraic complexity. In contrast, parameter identifiability is determined by the dimension of the image relative to the domain dimension p . If $\dim(\text{Im}(\Phi)) < p$, then by the Fiber Dimension Theorem (Hartshorne, 1977, Chapter 1), the fibers $\Phi^{-1}(f)$ are positive-dimensional varieties, and thus the network is defective. This comparison clarifies the trade-off: the ED degree depends on how small the image is inside \mathbb{R}^N , while identifiability depends on how compressed the map is from \mathbb{R}^p . A network can thus achieve low verification complexity while remaining non-identifiable if the architecture is over-parameterized.

3.2 Expected Real ED Degree

The results in the preceding section focus on critical points of the distance minimization problem over the complex field. For computation with homotopy continuation this is indeed the relevant quantity to consider. However, in some cases one may want to focus on the real critical points only. In practice, the number of real ED critical points is typically much smaller than the ED degree and may vary across different generic parameter realizations. To capture this behavior, we study the expected real ED degree, for a distribution of parameters. We leverage the Kac–Rice formalism (Kac, 1943; Rice, 1944) to derive a formula for this expectation, quantifying the typical number of real critical points encountered in robustness verification.

Theorem 3.10. *Let $f : \mathbb{R}^n \rightarrow \mathbb{R}$ be a random field that is almost surely twice continuously differentiable. Fix $\xi \in \mathbb{R}^n$ and, for $(\mathbf{x}, \lambda) \in \mathbb{R}^n \times (\mathbb{R} \setminus \{0\})$, define*

$$F(\mathbf{x}, \lambda) := \begin{pmatrix} f(\mathbf{x}) \\ \mathbf{x} - \xi + \lambda \nabla f(\mathbf{x}) \end{pmatrix}.$$

Assume that, for almost every (\mathbf{x}, λ) , the random vector $F(\mathbf{x}, \lambda)$ is nondegenerate⁴, that

$$\mathbb{P}(\det J_F(\mathbf{x}, \lambda) = 0 \mid F(\mathbf{x}, \lambda) = \mathbf{0}) = 0,$$

⁴By nondegenerate we mean that, for fixed (\mathbf{x}, λ) , the random vector $F(\mathbf{x}, \lambda)$ is not supported on any proper affine subspace of \mathbb{R}^{n+1} , equivalently that it admits a density with respect to Lebesgue measure on \mathbb{R}^{n+1} .

where $J_F(\mathbf{x}, \lambda)$ denotes the Jacobian matrix of F with respect to (\mathbf{x}, λ) , and that the integrand below is integrable on a region $U := U_{\mathbf{x}} \times U_{\lambda}$, with $U_{\lambda} \subset \mathbb{R} \setminus \{0\}$. Then

$$\mathbb{E}\left[\#\{(\mathbf{x}, \lambda) \in U : F(\mathbf{x}, \lambda) = \mathbf{0}\}\right] = \int_U |\lambda|^{-n} p_{(f(\mathbf{x}), \nabla f(\mathbf{x}))}(0, \frac{\xi - \mathbf{x}}{\lambda}) \mathcal{I}(\mathbf{x}, \lambda) d(\mathbf{x}, \lambda),$$

where $p_{(f(\mathbf{x}), \nabla f(\mathbf{x}))}$ is the joint density of $(f(\mathbf{x}), \nabla f(\mathbf{x}))$,

$$\mathcal{I}(\mathbf{x}, \lambda) = \mathbb{E}\left[\left|\nabla f(\mathbf{x})^\top \text{adj}(I_n + \lambda \nabla^2 f(\mathbf{x})) \nabla f(\mathbf{x})\right| \middle| f(\mathbf{x}) = 0, \nabla f(\mathbf{x}) = \frac{\xi - \mathbf{x}}{\lambda}\right],$$

with $\text{adj}(\cdot)$ the adjugate of a square matrix.

This gives the expected number of real critical points of the distance function from ξ to the random hypersurface defined by $f(\mathbf{x}) = 0$ within the set U . The formula is very general and necessarily involved. We can abstract away some of the details by considering NNGPs (Lee et al., 2018):

Corollary 3.11. *Let $f : \mathbb{R} \rightarrow \mathbb{R}$ be the neural network Gaussian process (NNGP) induced by an infinite-width two-layer network with polynomial activation of degree $d \geq 1$. Let $U = \mathbb{R} \times (\mathbb{R} \setminus \{0\})$. Then the expected real ED degree is*

$$\mathbb{E}\left[\#\{(\mathbf{x}, \lambda) \in U : F(\mathbf{x}, \lambda) = 0\}\right] = \frac{d}{\sqrt{2d-1}}.$$

Remark 3.12. In this one-dimensional case, by Proposition 3.2, an infinite-width two-layer network with degree- d activation has ED degree d , whereas on average only $\frac{d}{\sqrt{2d-1}}$ of these critical points are real. In contrast, for Kac polynomials of degree d , the expected number of real roots is about $O(\log d)$ (Breiding and Lerario, 2024). Thus, the special algebraic structure induced by the network parametrization significantly increases the expected number of real critical points compared to Kac polynomials.

4 Discriminants

In this section, we analyze the singular loci that govern transitions in verification complexity. We characterize the partition of the input space into regions of constant real critical point counts via the ED discriminant, and the stratification of the parameter space according to the algebraic degree of the decision boundary via the parameter discriminant. More precisely, we answer the following questions:

- (i) For fixed parameters θ , which test data points ξ yield fewer than the generic number of complex solutions?
- (ii) How does the ED degree of $\mathcal{V}_{c,c'}^\theta$ change as the network parameters θ vary?

4.1 ED Discriminant

In this subsection, we study the locus of data points that have fewer than the generic number of critical points when minimizing the distance to the decision boundary. For such data points, two distinct complex critical points collapse into a single critical point of higher multiplicity. This geometric degeneration marks the boundary where the number of real critical points changes; crossing this locus corresponds to the bifurcation event in the optimization landscape. We formalize this as the Euclidean distance discriminant.

Definition 4.1 (Euclidean Distance Discriminant). Let $\mathcal{V} \subset \mathbb{C}^n$ be an algebraic variety. The *Euclidean Distance (ED) discriminant* of \mathcal{V} , denoted by $\Sigma(\mathcal{V})$, is the Zariski closure of all data points $\mathbf{u} \in \mathbb{C}^n$ for which the critical points of the squared distance function $d_{\mathbf{u}}(\mathbf{x})$ on \mathcal{V} are not distinct. That is, $\Sigma(\mathcal{V})$ characterizes the data points for which the system has roots of multiplicity greater than one.

The notion of ED discriminant was introduced in the context of algebraic optimization by Draisma et al. (2016), and is also known as the *evolute*. It governs the stability of the optimization problem over the real numbers. In contrast with the number of complex critical points, which is generically constant, the number of real critical points is constant only on the connected components of $\mathbb{R}^n \setminus \Sigma(\mathcal{V})$.

Example 4.2. Consider a quadratic polynomial neural network with one hidden layer and architecture $(2, 2, 2)$. Fix parameter values $\theta = (W_1, \mathbf{b}_1, W_2, \mathbf{b}_2)$ with:

$$W_1 = \begin{pmatrix} 1 & 2 \\ 3 & 1 \end{pmatrix}, \mathbf{b}_1 = \begin{pmatrix} 0 \\ 1 \end{pmatrix}, W_2 = \begin{pmatrix} 2 & 1 \\ 1 & 2 \end{pmatrix}, \mathbf{b}_2 = \begin{pmatrix} 2 \\ 1 \end{pmatrix},$$

so the network output function f_θ becomes

$$(x_1, x_2) \mapsto \begin{bmatrix} f_{\theta,c} \\ f_{\theta,c'} \end{bmatrix} = \begin{bmatrix} 11x_1^2 + 14x_1x_2 + 9x_2^2 + 6x_1 + 2x_2 + 3 \\ 19x_1^2 + 16x_1x_2 + 6x_2^2 + 12x_1 + 4x_2 + 3 \end{bmatrix}.$$

The decision boundary defined by $B_\theta(\mathbf{x}) = f_{\theta,c}(\mathbf{x}) - f_{\theta,c'}(\mathbf{x})$ is a hyperbola. A computation in Macaulay2 (Grayson and Stillman) shows that $\mathcal{V}_{c,c'}^\theta$ has ED degree 4. The ED discriminant $\Sigma(\mathcal{V}_{c,c'}^\theta)$ is the variety in \mathbb{C}^2 defined as the set of zeros of a degree-6 polynomial $D \subseteq \mathbb{C}[u_1, u_2]$ in the data variables u_1 and u_2 :

$$\begin{aligned} D(u_1, u_2) = & 27u_1^6 + 54u_1^5u_2 - 180u_1^4u_2^2 - 280u_1^3u_2^3 + 480u_1^2u_2^4 + 384u_1u_2^5 - 512u_2^6 + 54u_1^5 \\ & + 180u_1^4u_2 - 120u_1^3u_2^2 - 720u_1^2u_2^3 + 768u_1^5 - 126u_1^4 + 582u_1^3u_2 - 2409u_1^2u_2^2 - 402u_1u_2^3 - 1371u_2^4 \\ & - 334u_1^3 + 1566u_1^2u_2 - 1878u_1u_2^2 + 808u_2^3 - 132u_1^2 + 1152u_1u_2 - 1218u_2^2 - 12u_1 + 516u_2 - 152. \end{aligned}$$

For all points $(u_1, u_2) \in \mathbb{R}^2$ with $D(u_1, u_2) \neq 0$, the number of distinct critical points of $d_u(\mathbf{x})$ on $\mathcal{V}_{c,c'}^\theta$ is 4, which can be real or complex, matching the ED degree.

On the other hand, for the test point $\mathbf{u} = (-2, 0)$ on the ED discriminant $D(\mathbf{u}) = 0$, the ideal $C_{c,c'}^\theta$ with respect to \mathbf{u} has a primary decomposition: $\langle 3x_1 + x_2 + 2, 25x_2^2 - 20x_2 + 4 \rangle \cap \langle 3x_1 - 4x_2 + 1, 25x_2^2 + 4x_2 - 2 \rangle$. The first ideal has one real solution $(-4/5, 2/5)$ with multiplicity 2. The second ideal has two real solutions. Geometrically, this marks a bifurcation in the optimization landscape: crossing the discriminant at \mathbf{u} changes the number of real critical points, as shown in Figure 3.

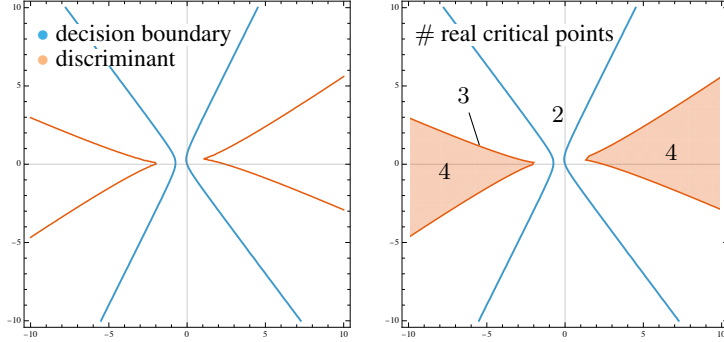


Figure 3: Left: The decision boundary is shown in blue and the corresponding ED discriminant curve is shown in orange. Right: The number of distinct real critical points of the distance minimization problem on different regions of the data space separated by the discriminant. The shaded region is where $D(u_1, u_2) > 0$.

Remark 4.3. The plot on the left shows the decision boundary in blue and the ED discriminant in orange. The plot on the right depicts the regions where $D > 0$ (shaded) and $D < 0$ (unshaded). Points in the unshaded (white) region, such as $(u_1, u_2) = (0, 0)$, have two real and two complex critical points, whereas points in the shaded region, such as $(10, 0)$ and $(-10, 0)$, have four real critical points. Along the separating curve $D = 0$ two complex critical points merge into a single real one; data points on this curve have three real critical points.

To generalize the idea in the above example, fix some parameters θ and let $B_\theta(\mathbf{x}) = f_{\theta,c}(\mathbf{x}) - f_{\theta,c'}(\mathbf{x})$ as before. The degree of the corresponding hypersurface can be arbitrarily large. In this case, we can compute the ED discriminant symbolically using Algorithm 2.

Intuition: Step 1 introduces the Lagrange multiplier λ to express the distance-minimization conditions algebraically. Step 2 encodes the critical-point equations $\mathbf{x} - \mathbf{u} = \lambda \nabla_{\mathbf{x}} B$ and $B_\theta(\mathbf{x}) = 0$. Step 3 forms the Jacobian of the critical-point system with respect to the variables (\mathbf{x}, λ) to detect when the correspondence between data points \mathbf{u} and critical points (\mathbf{x}, λ) ceases to be locally identifiable. Each solution (\mathbf{x}, λ) represents a critical point of the distance function for the given \mathbf{u} . When the Jacobian is invertible, these solutions depend smoothly on \mathbf{u} , which means that each critical point moves continuously as \mathbf{u} varies. When the Jacobian becomes singular, two or more critical points collide, or a critical point loses local uniqueness. These singular values of \mathbf{u} mark the onset of degeneracy in the optimization landscape and define the ED discriminant. Step 4 enforces this degeneracy by setting the determinant of the Jacobian to zero and removes trivial singularities

Algorithm 2 Symbolic computation of the ED discriminant

Require: Network parameters θ , classes (c, c')

Ensure: Ideal of the ED discriminant $\Sigma(\mathcal{V}_{c,c'}^\theta)$

1: Introduce a new variable λ and work over $\mathbb{Q}[\mathbf{x}, \mathbf{u}, \lambda]$.

2: Define

$$J_{c,c'}^\theta = I_{c,c'}^\theta + \langle x_i - u_i - \lambda \frac{\partial B}{\partial x_i} : i \in [n] \rangle.$$

3: Let $\text{Jac}_{c,c'}^\theta$ be the $n \times n$ Jacobian matrix of $J_{c,c'}^\theta$.

4: Define

$$C_{c,c'}^\theta = \left((I + \langle \det \text{Jac}_{c,c'}^\theta \rangle) : \langle n\text{-minors of } \text{Jac}_{c,c'}^\theta \rangle^\infty \right).$$

5: Compute the elimination ideal

$$E = C_{c,c'}^\theta \cap \mathbb{Q}[u_1, u_2].$$

6: **return** $D = \sqrt{E}$.

via saturation. Step 5 eliminates \mathbf{x} and λ , leaving only the condition on \mathbf{u} . The algorithm returns the radical to remove extra embedded components that may have arisen from elimination. The returned ideal defines the locus where the critical points merge and the number of distinct critical points drops below the ED degree.

Example 4.4. Consider again a quadratic neural network with one hidden layer and the architecture $(2, 2, 2)$. Slightly tweak the parameter values $\theta = (W_1, \mathbf{b}_1, W_2, \mathbf{b}_2)$ from the previous example:

$$W_1 = \begin{pmatrix} 1 & 2 \\ 3 & 1 \end{pmatrix}, \mathbf{b}_1 = \begin{pmatrix} 1 \\ 2 \end{pmatrix}, W_2 = \begin{pmatrix} 2 & 1 \\ 1 & 2 \end{pmatrix}, \mathbf{b}_2 = \begin{pmatrix} 1 \\ 1 \end{pmatrix},$$

A computation shows that in this case $\mathcal{V}_{c,c'}^\theta$ has ED degree 2. This is not surprising, since the quadratic form $B_\theta(\mathbf{x})$ is degenerate and factors into two linear terms:

$$B_\theta(x_1, x_2) = (x_2 - 2x_1 - 1)(4x_1 + 3x_2 + 3).$$

The ED discriminant is given by the following linear ideal

$$D(u_1, u_2) = \langle 5u_1 + 3, 5u_2 + 1 \rangle,$$

whose variety is a single point $\mathbf{u}^* = (-3/5, -1/5)$. At any other point \mathbf{u} , the ideal $C_{c,c'}^\theta$ has two distinct critical real points. However, at \mathbf{u}^* they collide, producing a single critical point. This critical point is \mathbf{u}^* itself, since it is on the model, i.e. $B_\theta(\mathbf{u}^*) = 0$.

The phenomenon observed in Example 4.4 generalizes to all reducible quadratic hypersurfaces of ED degree 2.

Proposition 4.5. *Let $\mathcal{V} = \{\mathbf{x} : \ell_1(\mathbf{x})\ell_2(\mathbf{x}) = 0\}$ be a reducible quadratic hypersurface consisting of two non-parallel hyperplanes. The ED degree of \mathcal{V} is 2. The two critical points collide if and only if the data \mathbf{u} lies on the intersection of the two hyperplanes $\ell_1(\mathbf{u}) = \ell_2(\mathbf{u}) = 0$. Consequently, the ED discriminant is contained in the model \mathcal{V} .*

4.2 Parameter Discriminant

In this section, we investigate how the complexity of the verification problem varies with the model parameters. Each parameter choice yields a decision boundary with an associated ED degree. The *parameter discriminant* is a locus in the parameter space where the ED degree drops below the generic value. As a result, this discriminant stratifies the parameter space into regions of constant ED degree.

We fix a shallow polynomial network with activation degree $d = 2$ and architecture (n, h, k) , and denote the polynomial defining the decision boundary as $B_\theta(\mathbf{x})$. Then $B_\theta(\mathbf{x})$ defines a quadric hypersurface in \mathbb{C}^n :

$$B_\theta(\mathbf{x}) = \mathbf{x}^\top A_\theta \mathbf{x} + \mathbf{b}_\theta^\top \mathbf{x} + c_\theta$$

for some symmetric matrix $A_\theta \in \mathbb{R}^{n \times n}$, vector $\mathbf{b}_\theta \in \mathbb{R}^n$, and scalar $c_\theta \in \mathbb{R}$ whose entries depend on θ . Let r be the number of distinct non-zero eigenvalues of A_θ and define the augmented matrix

$$M_\theta = \begin{pmatrix} A_\theta & \frac{1}{2}\mathbf{b}_\theta \\ \frac{1}{2}\mathbf{b}_\theta^\top & c_\theta \end{pmatrix}.$$

Theorem 4.6. *The ED degree of the decision boundary $\text{EDdegree}(\mathcal{V}_{c,c'}^\theta)$ is given by*

$$\begin{cases} 2r & \text{if } \text{rank}(M_\theta) = \text{rank}(A_\theta) + 1 \\ 2r + 1 & \text{if } \text{rank}(M_\theta) = \text{rank}(A_\theta) + 2 \\ 2r - 2 & \text{if } \text{rank}(M_\theta) = \text{rank}(A_\theta). \end{cases}$$

As a corollary, we characterize when the ED degree attains the generic value described in Proposition 3.2.

Corollary 4.7. *The ED degree $\text{EDdegree}(\mathcal{V}_{c,c'}^\theta)$ is exactly $2n$ if and only if all of the following hold:*

- A_θ is non-singular: $\text{rank}(A_\theta) = n$;
- $\mathcal{V}_{c,c'}^\theta$ is non-singular: $\text{rank}(M_\theta) = n + 1$;
- A_θ has distinct eigenvalues: the discriminant of the characteristic polynomial of A_θ is non-zero.

This implies that the ED degree drops strictly below $2n$ precisely when one of the generic conditions fails. This allows us to characterize the *parameter discriminant* algebraically:

Proposition 4.8. *The parameter discriminant $\mathcal{D} \subset \mathbb{R}^p$ is the hypersurface defined by the vanishing of the polynomial*

$$\Delta(\theta) = \det(A_\theta) \cdot \det(M_\theta) \cdot \text{Disc}_\lambda(\det(\lambda I - A_\theta)).$$

The set of parameters where $\text{EDdegree}(\mathcal{V}_{c,c'}^\theta) < 2n$ corresponds to the zero locus $\mathcal{D} = \{\theta \mid \Delta(\theta) = 0\}$.

The term $\text{Disc}_\lambda(\det(\lambda I - A_\theta))$ is the discriminant of the characteristic polynomial $P(\lambda) = \det(\lambda I - A_\theta)$ with respect to λ . This vanishes if and only if $P(\lambda)$ has multiple roots, meaning A_θ has repeated eigenvalues.

Remark 4.9. The discriminant \mathcal{D} is the union of three distinct components, each with a geometric meaning:

- $\det(A_\theta) = 0$: the quadratic form is rank-deficient, reducing the number of non-zero eigenvalues.
- $\det(M_\theta) = 0$: the decision boundary $\mathcal{V}_{c,c'}^\theta$ becomes singular as a variety.
- $\text{Disc}_\lambda = 0$: the matrix A_θ has repeated eigenvalues, so $r < n$ even if A_θ is full rank.

Conic sections We now specialize the preceding result to the case of $n = 2$ input variables, $\mathbf{x} = (x_1, x_2)^\top$. In this setting, the decision boundary is a *plane conic*, defined by

$$B_\theta(x_1, x_2) = ax_1^2 + bx_1x_2 + cx_2^2 + dx_1 + ex_2 + f = 0,$$

where the coefficients a, b, c, d, e, f depend on the parameters θ . The augmented matrix M_θ takes the form

$$M_\theta = \begin{pmatrix} a & b/2 & d/2 \\ b/2 & c & e/2 \\ d/2 & e/2 & f \end{pmatrix}, \quad \text{with} \quad A_\theta = \begin{pmatrix} a & b/2 \\ b/2 & c \end{pmatrix}.$$

Every plane conic belongs to one of the following types, determined by the algebraic properties of A_θ and M_θ :

- *Ellipse*: $\det(A_\theta) = ac - b^2/4 > 0$. ED degree is 4.
- *Hyperbola*: $\det A_\theta = ac - b^2/4 < 0$. ED degree is 4.
- *Parabola*: $\det A_\theta = ac - b^2/4 = 0$. ED degree is 3.
- *Circle*: A_θ has repeated eigenvalues ($a = c$ and $b = 0$). ED degree is 2.
- *Degenerate*: $\det M_\theta = 0$. ED degree is ≤ 2 .

Thus, the parameter discriminant \mathcal{D} for $n = 2$ is the union of the zero loci of three polynomials:

$$\Delta_{\text{sing}} = \det(M_\theta), \quad \Delta_{\text{par}} = ac - b^2/4, \quad \Delta_{\text{circ}} = (a - c)^2 + b^2.$$

The ED degree attains the generic value 4 if and only if all three polynomials are non-zero. For the geometry of the parameter discriminant \mathcal{D} in the ambient real space \mathbb{R}^6 :

- The loci $\{\Delta_{\text{par}} = 0\}$ and $\{\Delta_{\text{sing}} = 0\}$ are 5-dimensional hypersurfaces. They are boundaries between open regions of generic ellipses and hyperbolas.

- The circle locus $\{\Delta_{\text{circ}} = 0\}$ corresponds to the constraints $a = c$ and $b = 0$. This defines a 4-dimensional variety (real codimension 2) within the ellipse region.

This difference in dimension is illustrated in Figure 4. In a generic 2-dimensional cross-section of the parameter space, the codimension-1 hypersurfaces appear as curves, and the codimension-2 circle locus appears as a point.

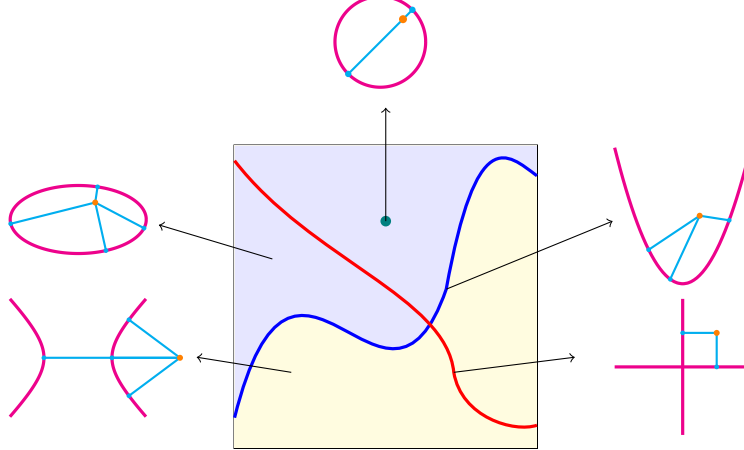


Figure 4: Schematic illustration of a 2D slice of the conic parameter space. Generic regions (ellipses/hyperbolas) have ED degree 4. The discriminant locus appears as a blue curve for parabolas and a red curve for singular conics, but as a green point for circles.

Now we return to the specific setting of a polynomial network with architecture $(2, 2, 2)$ trained as a binary classifier. For any fixed θ , the decision boundary is a plane conic. The geometry of this conic is determined via a polynomial map Φ from the parameter space (dim 12) to the conic coefficient space (dim 6). Explicitly, we have a conic $ax_1^2 + bx_1x_2 + \dots + f = 0$ whose coefficients are polynomials in θ :

$$\begin{aligned}
 a &= (w_{11}^{(1)})^2(w_{11}^{(2)} - w_{21}^{(2)}) + (w_{21}^{(1)})^2(w_{12}^{(2)} - w_{22}^{(2)}) \\
 b &= 2w_{11}^{(1)}w_{12}^{(1)}(w_{11}^{(2)} - w_{21}^{(2)}) + 2w_{21}^{(1)}w_{22}^{(1)}(w_{12}^{(2)} - w_{22}^{(2)}) \\
 c &= (w_{11}^{(1)})^2(w_{11}^{(2)} - w_{21}^{(2)}) + (w_{22}^{(1)})^2(w_{12}^{(2)} - w_{22}^{(2)}) \\
 d &= 2w_{11}^{(1)}b_1^{(1)}(w_{11}^{(2)} - w_{21}^{(2)}) + 2w_{21}^{(1)}(w_{12}^{(2)}b_2^{(1)} - w_{22}^{(2)}b_1^{(2)}) \\
 e &= 2w_{12}^{(1)}b_1^{(1)}(w_{11}^{(2)} - w_{21}^{(2)}) + 2w_{22}^{(1)}b_2^{(1)}(w_{12}^{(2)} - w_{22}^{(2)}) \\
 f &= (b_1^{(1)})^2(w_{11}^{(2)} - w_{21}^{(2)}) + (b_2^{(1)})^2(w_{12}^{(2)} - w_{22}^{(2)}) + b_1^{(2)} - b_2^{(2)}.
 \end{aligned}$$

As the parameters θ vary, the ED degree of the decision boundary is generically constant (equal to 4), but drops when the coefficients (a, \dots, f) lie on the discriminant locus \mathcal{D} . When $\Delta_{\text{par}} = 0$ while $\Delta_{\text{sing}} \neq 0$, the decision boundary is a parabola and the ED degree drops to 3. When $\Delta_{\text{circ}} = 0$, the boundary is a circle and the ED degree drops to 2. Finally, when $\Delta_{\text{sing}} = 0$, the decision boundary degenerates. The *parameter discriminant locus* for the neural network is therefore the preimage of the conic discriminant under Φ .

The algebraic characterization of the parameter discriminant could be used for complexity-aware model selection. By Corollary 4.7, strata with strictly lower ED degree are defined by the vanishing of specific polynomials. Thus, we may formulate an *algebraic regularizer* that targets a specific complexity class by augmenting the loss with a penalty term. For instance, $\mathcal{L}(\theta) + \lambda(\Delta_{\text{circ}}(\theta))^2$ would encourage models of lower algebraic complexity, trading generic expressivity for a decision boundary that is cheaper to verify.

5 Conclusion

We introduced an algebraic framework for robustness verification that connects neural network verification with tools from metric algebraic geometry. By characterizing verification through the Euclidean Distance

degree and associated discriminants, our results provide an architecture-, data-, and parameter-dependent notion of intrinsic verification complexity, enabling the identification of decision boundaries and test instances that are provably easier or harder to verify.

Our approach complements existing verification methods by offering exact, structure-aware guarantees and by clarifying how architectural, parametric, and data-dependent properties govern verification difficulty. This perspective suggests new directions for algorithm and architecture design that reduce verification complexity.

Important open directions remain. Our analysis focuses on Euclidean distance, and alternative metrics may reveal different complexity phenomena. Moreover, while our framework applies directly to polynomial classifiers, extending algebraic complexity measures and exact certification techniques to broader piecewise-algebraic or non-polynomial networks is an important challenge for future work.

Acknowledgments

This work was supported by the DARPA AIQ grant HR00112520014. GM was partially supported by the NSF grants DMS-2145630 and CCF-2212520, the DFG SPP 2298 grant 464109215, and the BMFTR in DAAD project 57616814 (SECAI).

References

Yulia Alexandr and Guido Montúfar. Constraining the outputs of ReLU neural networks, 2025. URL <https://arxiv.org/abs/2508.03867>.

Elizabeth S. Allman, Catherine Matias, and John A. Rhodes. Identifiability of parameters in latent structure models with many observed variables. *The Annals of Statistics*, 37(6A):3099–3132, 2009. ISSN 00905364, 21688966. URL <http://www.jstor.org/stable/25662188>.

Ross Anderson, Joey Huchette, Will Ma, Christian Tjandraatmadja, and Juan Pablo Vielma. Strong mixed-integer programming formulations for trained neural networks. *Mathematical Programming*, 183(1):3–39, 2020. doi: 10.1007/s10107-020-01474-5. URL <https://doi.org/10.1007/s10107-020-01474-5>.

D. N. Bernshtein. The number of roots of a system of equations. *Functional Analysis and Its Applications*, 9(3):183–185, 1975. doi: 10.1007/BF01075595.

Corinne Berzin, Alain Latour, and José León. Kac-Rice formula: A contemporary overview of the main results and applications, 2022. URL <https://arxiv.org/abs/2205.08742>.

Étienne Bézout. *Théorie générale des équations algébriques*. Paris, Impr. de Ph.-D. Pierres, Paris, 1779.

Elena Botoeva, Panagiotis Kouvaros, Jan Kronqvist, Alessio Lomuscio, and Ruth Misener. Efficient verification of ReLU-based neural networks via dependency analysis. *Proceedings of the AAAI Conference on Artificial Intelligence*, 34(04):3291–3299, 2020. doi: 10.1609/aaai.v34i04.5729. URL <https://ojs.aaai.org/index.php/AAAI/article/view/5729>.

Marie-Charlotte Brandenburg, Georg Loho, and Guido Montúfar. The real tropical geometry of neural networks for binary classification. *Transactions on Machine Learning Research*, 2024. ISSN 2835-8856. URL <https://openreview.net/forum?id=I7JWf8XA2w>.

Paul Breiding and Antonio Lerario. Random algebraic geometry, 2024. URL <https://pbrdng.github.io/rag.pdf>. Book draft.

Paul Breiding and Sascha Timme. Homotopycontinuation.jl: A package for homotopy continuation in Julia. In *Proc. ICMS*, pages 458–465, 2018.

Paul Breiding, Kathlén Kohn, and Bernd Sturmfels. *Metric Algebraic Geometry*. Oberwolfach Seminars. Birkhäuser Cham, 1 edition, 2024. ISBN 978-3-031-51461-6. doi: 10.1007/978-3-031-51462-3.

Christopher Brix, Mark Niklas Müller, Stanley Bak, Taylor T. Johnson, and Changliu Liu. First three years of the international verification of neural networks competition (VNN-COMP). *International Journal on Software Tools for Technology Transfer*, 25(3):329–339, 2023. doi: 10.1007/s10009-023-00703-4.

Nicholas Carlini and David Wagner. Towards evaluating the robustness of neural networks. In *2017 IEEE Symposium on Security and Privacy (SP)*, pages 39–57, Los Alamitos, CA, USA, 2017. IEEE Computer Society. doi: 10.1109/SP.2017.49. URL <https://doi.ieee.org/10.1109/SP.2017.49>.

Jan Draisma, Emil Horobeț, Giorgio Ottaviani, Bernd Sturmfels, and Rekha R. Thomas. The Euclidean Distance Degree of an Algebraic Variety. *Foundations of Computational Mathematics*, 16(1):99–149, 2016. doi: 10.1007/s10208-014-9240-x. URL <https://doi.org/10.1007/s10208-014-9240-x>.

Timothy Duff, Cvetelina Hill, Anders Jensen, Kisun Lee, Anton Leykin, and Jeff Sommars. Solving polynomial systems via homotopy continuation and monodromy. *IMA Journal of Numerical Analysis*, 39(3):1421–1446, 2018. doi: 10.1093/imanum/dry017. URL <https://doi.org/10.1093/imanum/dry017>.

James Ferlez and Yasser Shoukry. Bounding the complexity of formally verifying neural networks: A geometric approach. In *2021 60th IEEE Conference on Decision and Control (CDC)*, pages 5104–5109, 2021. doi: 10.1109/CDC45484.2021.9683375.

Vincent Froese, Moritz Grillo, and Martin Skutella. Complexity of injectivity and verification of ReLU neural networks. In Nika Haghtalab and Ankur Moitra, editors, *Proceedings of Thirty Eighth Conference on Learning Theory*, volume 291 of *Proceedings of Machine Learning Research*, pages 2188–2189. PMLR, 2025. URL <https://proceedings.mlr.press/v291/froese25a.html>.

Timon Gehr, Matthew Mirman, Dana Drachsler-Cohen, Petar Tsankov, Swarat Chaudhuri, and Martin Vechev. Ai2: Safety and robustness certification of neural networks with abstract interpretation. In *2018 IEEE Symposium on Security and Privacy (SP)*, pages 3–18, 2018. doi: 10.1109/SP.2018.00058.

Daniel R. Grayson and Michael E. Stillman. Macaulay2, a software system for research in algebraic geometry. Available at <http://www2.macaulay2.com>.

Robin Hartshorne. *Algebraic geometry.*, volume 52 of *Graduate texts in mathematics*. Springer, 1977.

Matthias Hein and Maksym Andriushchenko. Formal guarantees on the robustness of a classifier against adversarial manipulation. In *Advances in Neural Information Processing Systems*, volume 30. Curran Associates, Inc., 2017. URL https://proceedings.neurips.cc/paper_files/paper/2017/file/e077e1a544eec4f0307cf5c3c721d944-Paper.pdf.

Nathan W. Henry, Giovanni Luca Marchetti, and Kathlén Kohn. Geometry of lightning self-attention: Identifiability and dimension. In *The Thirteenth International Conference on Learning Representations*, 2025. URL <https://openreview.net/forum?id=XtY3xYQWcW>.

Leon Isserlis. On a formula for the product-moment coefficient of any order of a normal frequency distribution in any number of variables. *Biometrika*, 12(1–2):134–139, 1918. doi: 10.1093/biomet/12.1-2.134. URL <https://doi.org/10.1093/biomet/12.1-2.134>.

Svante Janson. *Gaussian Hilbert Spaces*. Cambridge Tracts in Mathematics. Cambridge University Press, Cambridge, 1997.

M. Kac. On the average number of real roots of a random algebraic equation. *Bulletin of the American Mathematical Society*, 49(4):314–320, 1943.

W. Karush. Minima of functions of several variables with inequalities as side conditions. Master’s thesis, University of Chicago, Department of Mathematics, 1939.

Guy Katz, Clark Barrett, David L. Dill, Kyle Julian, and Mykel J. Kochenderfer. Reluplex: An efficient smt solver for verifying deep neural networks. In *Computer Aided Verification*, pages 97–117, Cham, 2017. Springer International Publishing. doi: 10.1007/978-3-319-63387-9_5.

A. G. Khovanskii. Newton polyhedra and the genus of complete intersections. *Functional Analysis and Its Applications*, 12(1):38–46, 1978. doi: 10.1007/BF01077562.

Joe Kileel, Matthew Trager, and Joan Bruna. On the expressive power of deep polynomial neural networks. In *Advances in Neural Information Processing Systems*, volume 32. Curran Associates, Inc., 2019. URL https://proceedings.neurips.cc/paper_files/paper/2019/file/a0dc078ca0d99b5ebb465a9f1cad54ba-Paper.pdf.

Diederik P. Kingma and Jimmy Ba. Adam: A method for stochastic optimization. In *ICLR (Poster)*, 2015. URL <http://arxiv.org/abs/1412.6980>.

Kathlén Kohn, Thomas Merkh, Guido Montúfar, and Matthew Trager. Geometry of linear convolutional networks. *SIAM Journal on Applied Algebra and Geometry*, 6(3):368–406, 2022. doi: 10.1137/21M1441183. URL <https://doi.org/10.1137/21M1441183>.

Matthias König, Annelot W. Bosman, Holger H. Hoos, and Jan N. van Rijn. Critically assessing the state of the art in neural network verification. *Journal of Machine Learning Research*, 25(12):1–53, 2024. URL <http://jmlr.org/papers/v25/23-0119.html>.

Kaie Kubjas, Jiayi Li, and Maximilian Wiesmann. Geometry of polynomial neural networks. *Algebraic Statistics*, 15(2):295–328, 2024. ISSN 2693-2997. doi: 10.2140/astat.2024.15.295. URL <http://dx.doi.org/10.2140/astat.2024.15.295>.

Harold W. Kuhn and Albert W. Tucker. Nonlinear programming. In *Traces and Emergence of Nonlinear Programming*, pages 247–258. Springer Basel, Basel, 2014. doi: 10.1007/978-3-0348-0439-4_11. URL https://doi.org/10.1007/978-3-0348-0439-4_11.

A. G. Kushnirenko. Newton polytopes and the Bezout theorem. *Functional Analysis and Its Applications*, 10(3):233–235, 1976. doi: 10.1007/BF01075534.

Zehua Lai, Lek-Heng Lim, and Ke Ye. Euclidean distance degree in manifold optimization. *SIAM Journal on Optimization*, 35(4):2402–2422, 2025. doi: 10.1137/25M1735032. URL <https://doi.org/10.1137/25M1735032>.

Hwangrae Lee. The Euclidean distance degree of Fermat hypersurfaces. *Journal of Symbolic Computation*, 79:318–328, 2017.

Jaehoon Lee, Jascha Sohl-Dickstein, Jeffrey Pennington, Roman Novak, Sam Schoenholz, and Yasaman Bahri. Deep neural networks as Gaussian processes. In *International Conference on Learning Representations*, 2018. URL <https://openreview.net/forum?id=B1EA-M-0Z>.

T. Y. Li. Numerical solution of multivariate polynomial systems by homotopy continuation methods. *Acta Numerica*, 6:399–436, 1997. doi: 10.1017/S0962492900002749.

Jiaxiang Liu, Yunhan Xing, Xiaomu Shi, Fu Song, Zhiwu Xu, and Zhong Ming. Abstraction and refinement: Towards scalable and exact verification of neural networks. *ACM Trans. Softw. Eng. Methodol.*, 33(5), 2024. doi: 10.1145/3644387. URL <https://doi.org/10.1145/3644387>.

Laurentiu G. Maxim, Jose I. Rodriguez, and Botong Wang. Euclidean distance degree of the multiview variety. *SIAM Journal on Applied Algebra and Geometry*, 4(1):28–48, 2020. doi: 10.1137/18M1233406. URL <https://doi.org/10.1137/18M1233406>.

Mark Huasong Meng, Guangdong Bai, Sin Gee Teo, Zhe Hou, Yan Xiao, Yun Lin, and Jin Song Dong. Adversarial robustness of deep neural networks: A survey from a formal verification perspective. *IEEE Transactions on Dependable and Secure Computing*, pages 1–1, 2022. doi: 10.1109/TDSC.2022.3179131.

Aditi Raghunathan, Jacob Steinhardt, and Percy Liang. Certified defenses against adversarial examples. In *International Conference on Learning Representations*, 2018. URL <https://openreview.net/forum?id=Bys4ob-Rb>.

S. O. Rice. Mathematical analysis of random noise. *The Bell System Technical Journal*, 23(3):282–332, 1944. doi: 10.1002/j.1538-7305.1944.tb00874.x.

Hadi Salman, Greg Yang, Huan Zhang, Cho-Jui Hsieh, and Pengchuan Zhang. A convex relaxation barrier to tight robustness verification of neural networks. In *Advances in Neural Information Processing Systems*, volume 32. Curran Associates, Inc., 2019. URL https://proceedings.neurips.cc/paper_files/paper/2019/file/246a3c5544feb054f3ea718f61adfa16-Paper.pdf.

Gagandeep Singh, Timon Gehr, Matthew Mirman, Markus Püschel, and Martin Vechev. Fast and effective robustness certification. In *Advances in Neural Information Processing Systems*, volume 31. Curran Associates, Inc., 2018. URL https://proceedings.neurips.cc/paper_files/paper/2018/file/f2f446980d8e971ef3da97af089481c3-Paper.pdf.

Andrew J Sommese and Charles W Wampler. *The Numerical Solution of Systems of Polynomials Arising in Engineering and Science*. WORLD SCIENTIFIC, 2005. doi: 10.1142/5763. URL <https://www.worldscientific.com/doi/abs/10.1142/5763>.

Andrew J. Sommese, Jan Verschelde, and Charles W. Wampler. Numerical decomposition of the solution sets of polynomial systems into irreducible components. *SIAM Journal on Numerical Analysis*, 38(6):2022–2046, 2001. doi: 10.1137/S0036142900372549. URL <https://doi.org/10.1137/S0036142900372549>.

Andrew J. Sommese, Jan Verschelde, and Charles W. Wampler. Introduction to numerical algebraic geometry. In *Solving Polynomial Equations: Foundations, Algorithms, and Applications*, volume 14 of *Algorithms and Computation in Mathematics*, pages 301–337. Springer, Berlin, Heidelberg, 2005.

Christian Szegedy, Wojciech Zaremba, Ilya Sutskever, Joan Bruna, Dumitru Erhan, Ian Goodfellow, and Rob Fergus. Intriguing properties of neural networks, 2014. URL <https://arxiv.org/abs/1312.6199>.

Vincent Tjeng, Kai Y. Xiao, and Russ Tedrake. Evaluating robustness of neural networks with mixed integer programming. In *International Conference on Learning Representations*, 2019. URL <https://openreview.net/forum?id=HyGIdiRqtM>.

Konstantin Usevich, Ricardo Augusto Borsoi, Clara Dérand, and Marianne Clausel. Identifiability of deep polynomial neural networks. In *The Thirty-ninth Annual Conference on Neural Information Processing Systems*, 2025. URL <https://openreview.net/forum?id=MrUsZfQ9pC>.

Luca Venturi, Afonso S. Bandeira, and Joan Bruna. Spurious valleys in one-hidden-layer neural network optimization landscapes. *Journal of Machine Learning Research*, 20(133):1–34, 2019. URL <http://jmlr.org/papers/v20/18-674.html>.

Lily Weng, Huan Zhang, Hongge Chen, Zhao Song, Cho-Jui Hsieh, Luca Daniel, Duane Boning, and Inderjit Dhillon. Towards fast computation of certified robustness for ReLU networks. In *Proceedings of the 35th International Conference on Machine Learning*, volume 80 of *Proceedings of Machine Learning Research*, pages 5276–5285. PMLR, 2018. URL <https://proceedings.mlr.press/v80/weng18a.html>.

Eric Wong and Zico Kolter. Provable defenses against adversarial examples via the convex outer adversarial polytope. In *Proceedings of the 35th International Conference on Machine Learning*, volume 80 of *Proceedings of Machine Learning Research*, pages 5286–5295. PMLR, 2018. URL <https://proceedings.mlr.press/v80/wong18a.html>.

Huan Zhang, Tsui-Wei Weng, Pin-Yu Chen, Cho-Jui Hsieh, and Luca Daniel. Efficient neural network robustness certification with general activation functions. In *Advances in Neural Information Processing Systems*, volume 31. Curran Associates, Inc., 2018. URL https://proceedings.neurips.cc/paper_files/paper/2018/file/d04863f100d59b3eb688a11f95b0ae60-Paper.pdf.

Xingjian Zhou, Keyi Shen, Andy Xu, Hongji Xu, Cho-Jui Hsieh, Huan Zhang, and Zhouxing Shi. Soundness-bench: A soundness benchmark for neural network verifiers. *Transactions on Machine Learning Research*, 2025. ISSN 2835-8856. URL <https://openreview.net/forum?id=UuYYldVLH3>.

Appendix A Numerical Solution via Homotopy Continuation

Homotopy continuation is a standard numerical method in numerical algebraic geometry for solving polynomial systems by tracking solution paths through a family of embeddings. We employ this technique to compute all critical points of the distance minimization Problem 5.

A.1 Formulation and the Gamma Trick

Let $F(\mathbf{z}) = (F_1(\mathbf{z}), \dots, F_m(\mathbf{z})) : \mathbb{C}^m \rightarrow \mathbb{C}^m$ be a polynomial system with m equations in m unknowns. For generic coefficients, the solution set $F(\mathbf{z}) = \mathbf{0}$ consists of finitely many isolated points, whose cardinality is bounded above by the Bézout bound (Bézout, 1779) and more precisely by the Bernstein–Kushnirenko–Khovanskii (BKK) bound (Bernshtein, 1975; Kushnirenko, 1976; Khovanskii, 1978).

The core idea of homotopy continuation is to embed F into a family of polynomial systems parametrized by $t \in [0, 1]$:

$$H(\mathbf{z}, t; \gamma) := \gamma(1 - t)G(\mathbf{z}) + tF(\mathbf{z}),$$

where $G(\mathbf{z})$ is a *start system* with known solutions and the same monomial support as F , and $\gamma \in \mathbb{C}^*$ is a generic nonzero complex scalar. We apply the gamma trick to ensure with probability one that all solution paths remain smooth and non-singular throughout $t \in (0, 1)$ by choosing γ as a generic random complex number. This crucial step avoids path crossing or singularities that could arise from degeneracies in the coefficient structure. For almost all choices of γ , each solution \mathbf{z}_0 of the start system $G(\mathbf{z}) = \mathbf{0}$ lifts to a unique solution path $\mathbf{z}(t)$ satisfying

$$H(\mathbf{z}(t), t; \gamma) = \mathbf{0}, \quad \mathbf{z}(0) = \mathbf{z}_0, \quad \mathbf{z}(1) \in \{\text{solutions of } F(\mathbf{z}) = \mathbf{0}\}.$$

By tracking all solution paths from $t = 0$ to $t = 1$, we obtain all solutions of the target system.

A.2 Path Tracking via Predictor–Corrector Methods

Numerical path tracking discretizes the parameter t and alternates between prediction and correction steps to maintain accuracy. Differentiating the homotopy equation $H(\mathbf{z}(t), t; \gamma) = \mathbf{0}$ along a solution path yields the *Davidenko equation*:

$$\frac{d\mathbf{z}}{dt} = -(\nabla_{\mathbf{z}} H(\mathbf{z}(t), t; \gamma))^{-1} \frac{\partial H}{\partial t}(\mathbf{z}(t), t; \gamma),$$

provided the Jacobian matrix $\nabla_{\mathbf{z}} H$ remains nonsingular along the path.

Given a current point (\mathbf{z}_k, t_k) , the *prediction step* advances to the next parameter value $t_{k+1} = t_k + \Delta t$ using a first-order Euler tangent predictor:

$$\mathbf{z}_{k+1}^{\text{pred}} = \mathbf{z}_k - \Delta t (\nabla_{\mathbf{z}} H(\mathbf{z}_k, t_k; \gamma))^{-1} \frac{\partial H}{\partial t}(\mathbf{z}_k, t_k; \gamma).$$

The predicted point is then refined using a *correction step*, typically Newton’s method applied to $H(\mathbf{z}, t_{k+1}; \gamma) = \mathbf{0}$:

$$\mathbf{z}^{(\ell+1)} = \mathbf{z}^{(\ell)} - (\nabla_{\mathbf{z}} H(\mathbf{z}^{(\ell)}, t_{k+1}; \gamma))^{-1} H(\mathbf{z}^{(\ell)}, t_{k+1}; \gamma),$$

initialized at $\mathbf{z}^{(0)} = \mathbf{z}_{k+1}^{\text{pred}}$ and iterated until convergence. Adaptive step-size control ensures that Δt is reduced if the corrector fails to converge or residuals stagnate, maintaining numerical stability and efficiency. Higher-order predictors and extrapolation strategies may be employed for improved robustness on ill-conditioned systems.

A.3 Implementation and Post-Processing

Our implementation builds upon the `HomotopyContinuation.jl` package (Breiding and Timme, 2018), which provides robust path tracking with automatic step-size adaptation, endgaming strategies for finite solutions, and detection of solutions at infinity. After tracking all paths to $t = 1$, we retain only the *real solutions* satisfying $\|\text{Im}(\mathbf{z})\| < \epsilon_{\text{tol}}$ for a tolerance threshold ϵ_{tol} . Among the feasible real solutions, we select the one minimizing the distance function $d_{\xi}(x)$ to obtain the certified robustness margin.

Appendix B Proofs

B.1 Proof of Proposition 2.1

Proposition 2.1. *Let $f_{\theta} : \mathbb{R}^n \rightarrow \mathbb{R}^k$ be a continuous classifier, and let $\hat{c}(\mathbf{x}) := \arg \max_{i \in [k]} f_{\theta,i}(\mathbf{x})$ denote the predicted class. Fix a test point $\xi \in \mathbb{R}^n$ and write $c := \hat{c}(\xi)$. Assume that the prediction at ξ is unique, i.e.,*

$$f_{\theta,c}(\xi) > f_{\theta,c'}(\xi) \quad \text{for all } c' \neq c.$$

Then, for γ and $\tilde{\gamma}$ defined in (1) and (4), we have $\gamma = \tilde{\gamma}$.

Proof. First, it is clear that $\tilde{\gamma} \leq \gamma$ since $\mathcal{B}_{c,c'}^{\theta} \subseteq \mathcal{V}_{c,c'}^{\theta}$. Now we show the reverse inequality. For the relaxed problem, assume that the infimum is attained at $\mathbf{x}^* \in \mathcal{V}_{c,c^*}^{\theta}$ for some $c^* \neq c$ such that $d_{\xi}(\mathbf{x}^*) = \tilde{\gamma}^2$.

Let ℓ be a class other than c that achieves the maximum logit at \mathbf{x}^* , i.e. $f_{\theta,\ell}(\mathbf{x}^*) = \max_i f_{\theta,i}(\mathbf{x}^*)$ and $\ell \neq c$. If $\ell = c^*$, then \mathbf{x}^* lies on an active decision boundary between class c and class c^* . Therefore $\gamma \leq d_{\xi}(\mathbf{x}^*) = \tilde{\gamma}$, which establishes $\gamma \leq \tilde{\gamma}$. It remains to rule out the case $\ell \neq c^*$. Suppose, for contradiction, that $f_{\theta,\ell}(\mathbf{x}^*) > f_{\theta,c}(\mathbf{x}^*)$ for some $\ell \neq c^*$. Consider the line segment between ξ and \mathbf{x}^* ,

$$\mathbf{x}(t) := (1-t)\xi + t\mathbf{x}^*, \quad t \in [0, 1],$$

and the continuous function $g : \mathbb{R} \rightarrow \mathbb{R}$,

$$g(t) := f_{\theta,c}(\mathbf{x}(t)) - f_{\theta,\ell}(\mathbf{x}(t)).$$

At $t = 0$, we have $g(0) = f_{\theta,c}(\xi) - f_{\theta,\ell}(\xi) > 0$ by uniqueness of the maximizer c at ξ . At $t = 1$, we have $g(1) = f_{\theta,c}(\mathbf{x}^*) - f_{\theta,\ell}(\mathbf{x}^*) < 0$ by assumption. By the intermediate value theorem, there exists $t^* \in (0, 1)$ such that $g(t^*) = 0$, i.e.

$$f_c(\mathbf{x}(t^*)) = f_{\ell}(\mathbf{x}(t^*)).$$

Let $\mathbf{z} := \mathbf{x}(t^*)$. Then $\mathbf{z} \in \mathcal{V}_{c,\ell}^{\theta}$, and since \mathbf{z} lies strictly between ξ and \mathbf{x}^* on the segment,

$$\sqrt{d_{\xi}(\mathbf{z})} = t \sqrt{d_{\xi}(\mathbf{x}^*)} < \sqrt{d_{\xi}(\mathbf{x}^*)} = \tilde{\gamma}.$$

This contradicts the definition of $\tilde{\gamma}$ as the minimum distance from ξ to $\mathcal{V}_{c,c'}^{\theta}$ for all $c' \neq c$. Therefore, we must have $\ell = c^*$, and hence $\gamma \leq \tilde{\gamma}$. Combining both inequalities, we conclude that $\gamma = \tilde{\gamma}$. This completes the proof. \square

B.2 Proof of Proposition 3.2

Proposition 3.2. *Consider a neural network with architecture (n, h, k) and a degree- d polynomial activation function. Assume the parameters θ are generic. The ED degree of the decision boundary $\mathcal{V}_{c,c'}^{\theta}$ is given by*

$$\text{EDdegree}(\mathcal{V}_{c,c'}^{\theta}) = d \sum_{i=0}^{m-1} (d-1)^i, \quad \text{where } m = \min\{n, h\}.$$

Proof. The decision boundary is defined by the polynomial $B_{\theta}(\mathbf{x}) = f_{\theta,c}(\mathbf{x}) - f_{\theta,c'}(\mathbf{x})$. Since the network has a single hidden layer with width h and a degree- d polynomial activation $\sigma(z) = z^d$, the function $B_{\theta}(\mathbf{x})$ takes the form

$$B_{\theta}(\mathbf{x}) = \sum_{j=1}^h \alpha_j (\mathbf{w}_j^T \mathbf{x} + b_j)^d + \beta,$$

where $\mathbf{w}_j \in \mathbb{R}^n$ are the rows of the first layer weight matrix $W^{(1)} \in \mathbb{R}^{h \times n}$, and $b_j \in \mathbb{R}$ are the entries of the first layer bias vector $\mathbf{b}^{(1)} \in \mathbb{R}^h$. The coefficients are given by $\alpha_j = W_{j,c}^{(2)} - W_{j,c'}^{(2)}$ and $\beta = b_c^{(2)} - b_{c'}^{(2)}$, where $W^{(2)} \in \mathbb{R}^{h \times k}$ is the output layer weight matrix and $\mathbf{b}^{(2)} \in \mathbb{R}^k$ is the output bias vector. We analyze the ED degree of $\mathcal{V}_{c,c'}^{\theta}$ in two cases based on the relationship between n and h .

First, assume $n \leq h$. Since the parameters θ are generic, $B_{\theta}(\mathbf{x})$ is a weighted sum of n linearly independent powers, which identifies $\mathcal{V}_{c,c'}^{\theta}$ as a generic scaled Fermat hypersurface. Following Lee (2017, Section 3), the

Euclidean distance degree of a generic scaled Fermat hypersurface is equal to that of a generic hypersurface in \mathbb{C}^n . [Draisma et al. \(2016, Proposition 2.6\)](#) show the ED degree for a generic hypersurface of degree d in n variables is

$$\text{ED degree}(\mathcal{V}_{c,c'}^\theta) = d \sum_{i=0}^{n-1} (d-1)^i,$$

as desired.

Now, suppose $n > h$. Let $W = \text{span}\{\mathbf{w}_1, \dots, \mathbf{w}_h\} \subset \mathbb{R}^n$ be the subspace spanned by the weight vectors. Since the parameters θ are generic and $h < n$, the vectors $\mathbf{w}_1, \dots, \mathbf{w}_h$ are linearly independent, so $\dim(W) = h$. We perform an orthogonal change of coordinates $\mathbf{x} = Q\mathbf{y}$, where $Q \in \mathbb{R}^{n \times n}$ is an orthogonal matrix constructed such that its first h columns form a basis for W .

In this new coordinate system, for every $j \in \{1, \dots, h\}$, the vector \mathbf{w}_j lies entirely within the span of the first h basis vectors. Consequently, the inner product $\mathbf{w}_j^T \mathbf{x}$ depends exclusively on the first h coordinates y_1, \dots, y_h . The polynomial $B_\theta(\mathbf{x})$ can thus be written as

$$B_\theta(Q\mathbf{y}) = \tilde{B}_\theta(y_1, \dots, y_h),$$

where \tilde{B}_θ is a generic scaled Fermat polynomial of degree d in h variables. This implies that the variety $\mathcal{V}_{c,c'}^\theta$ decomposes as:

$$\mathcal{V}_{c,c'}^\theta \cong \mathcal{Z} \times \mathbb{C}^{n-h},$$

where $\mathcal{Z} = \{z \in \mathbb{C}^h \mid \tilde{B}_\theta(z) = 0\}$ is a generic hypersurface in \mathbb{C}^h .

The squared Euclidean distance from a generic data point \mathbf{u} , transformed to $\tilde{\mathbf{u}} = Q^T \mathbf{u}$, splits into two independent terms:

$$d_{\mathbf{u}}(\mathbf{x}) = d_{\tilde{\mathbf{u}}}(\mathbf{y}) = \sum_{i=1}^h (y_i - \tilde{u}_i)^2 + \sum_{i=h+1}^n (y_i - \tilde{u}_i)^2.$$

To find the ED degree, we determine the number of critical points of this distance function on the variety. The second term depends only on y_{h+1}, \dots, y_n , which are unconstrained by \tilde{B}_θ . This term has exactly one critical point (the global minimum) at $y_i = \tilde{u}_i$ for all $i > h$. The first term seeks critical points of the distance to the hypersurface \mathcal{Z} in \mathbb{C}^h . Since \mathcal{Z} is defined by a generic polynomial of degree d in h variables, by [Draisma et al. \(2016, Proposition 2.6\)](#), the number of such points is $d \sum_{i=0}^{h-1} (d-1)^i$. The total ED degree of $\mathcal{V}_{c,c'}^\theta$ is the product of these counts, and the conclusion follows. \square

B.3 Proof of Proposition 3.6

Proposition 3.6. *Consider a deep neural network with architecture $(n, h_1, 1, \dots, 1, k)$ having s hidden layers and degree- d activation. Assume $h_1 \geq n$ and generic θ . Then*

$$\text{EDdegree}(\mathcal{V}_{c,c'}^\theta) = D \sum_{i=0}^{n-1} (d-1)^i,$$

where $D = d^s$ is the total composite degree of the network.

Proof. The first hidden layer $h_1 \geq n$ produces a generic multivariate polynomial $P(\mathbf{x})$. The subsequent $k-1$ hidden layers of width 1 compute a univariate polynomial $G(t)$ of degree d^{s-1} , evaluated at $t = P(\mathbf{x})$. The final output layer is linear, so the decision boundary $B_\theta(\mathbf{x}) = f_c(\mathbf{x}) - f_{c'}(\mathbf{x}) = 0$ is given by:

$$(\alpha_c - \alpha_{c'})G(P(\mathbf{x})) + (\beta_c - \beta_{c'}) = 0.$$

Let $\Delta\alpha = \alpha_c - \alpha_{c'}$ and $\Delta\beta = \beta_c - \beta_{c'}$. For generic weights, $\Delta\alpha \neq 0$. We must solve:

$$G(P(\mathbf{x})) = -\frac{\Delta\beta}{\Delta\alpha}.$$

The univariate equation $G(t) = -\Delta\beta/\Delta\alpha$ has $M = d^{s-1}$ distinct roots $\{\lambda_1, \dots, \lambda_M\}$. This implies that the decision boundary decomposes into M disjoint hypersurfaces defined by $P(\mathbf{x}) = \lambda_j$. Since these are parallel

copies of the generic base surface $P(\mathbf{x}) = 0$, the total ED degree is the sum of their individual ED degrees. The ED degree of a generic degree- d hypersurface in n variables is $d \sum_{i=0}^{n-1} (d-1)^i$. Multiplying this by M yields:

$$\text{EDdegree}(\mathcal{V}_{c,c'}^\theta) = d^{s-1} \cdot \left[d \sum_{i=0}^{n-1} (d-1)^i \right] = d^s \sum_{i=0}^{n-1} (d-1)^i.$$

□

B.4 Proof of Proposition 3.8

Proposition 3.8. *Consider a deep neural network with architecture (n, h_1, \dots, h_s, k) . Assume degree- d activation, and $h_i \geq n$ for all $i \in [s]$. For generic parameters θ ,*

$$\text{ED degree}(\mathcal{V}_{c,c'}^\theta) = D \sum_{i=0}^{n-1} (D-1)^i,$$

where $D = d^s$ is the composite degree of the network.

Proof. The Euclidean Distance degree is a lower semi-continuous function on the irreducible parameter space, so the generic value is the maximum attainable value. As pointed out by [Draisma et al. \(2016\)](#), the ED degree of a degree- D hypersurface is bounded by $D \sum_{i=0}^{n-1} (D-1)^i$, with equality holding if the hypersurface is smooth and intersects the isotropic quadric at infinity transversally.

To prove the proposition, it suffices to construct a single parameter configuration θ^* such that the decision boundary defines a hypersurface achieving this bound. Since $h_i \geq n$ for all $i \in [s]$, we can enforce n disjoint computational paths by setting the weights of each hidden layer to be a block matrix with the $n \times n$ identity in the top-left corner and zeros elsewhere:

$$W^{(i)} = \begin{bmatrix} I_n & \mathbf{0} \\ \mathbf{0} & \mathbf{0} \end{bmatrix}.$$

Setting all hidden biases to zero, this configuration maps the input \mathbf{x} to the vector (x_1^D, \dots, x_n^D) at the final hidden layer. For the output layer weights $W^{(s+1)} \in \mathbb{C}^{k \times h_s}$, let $\mathbf{w}_c, \mathbf{w}_{c'}$ denote the two rows corresponding to c and c' . We choose weights such that their difference $\mathbf{w}_{\text{diff}} = \mathbf{w}_c - \mathbf{w}_{c'}$ has generic entries $\lambda_1, \dots, \lambda_n$ in the first n positions and zero otherwise. The decision boundary becomes the scaled Fermat polynomial:

$$f_1(\mathbf{x}) - f_2(\mathbf{x}) = \sum_{j=1}^n \lambda_j x_j^D - C = 0.$$

For generic λ_j , this hypersurface is smooth and transversal to the isotropic quadric $\sum x_j^2 = 0$ at infinity ([Lee, 2017](#)). Thus, the witness achieves the maximal ED degree. Since the network can realize a maximal instance, the generic network achieves the maximal count. □

B.5 Proof of Theorem 3.10

Theorem 3.10. *Let $f : \mathbb{R}^n \rightarrow \mathbb{R}$ be a random field that is almost surely twice continuously differentiable. Fix $\xi \in \mathbb{R}^n$ and, for $(\mathbf{x}, \lambda) \in \mathbb{R}^n \times (\mathbb{R} \setminus \{0\})$, define*

$$F(\mathbf{x}, \lambda) := \begin{pmatrix} f(\mathbf{x}) \\ \mathbf{x} - \xi + \lambda \nabla f(\mathbf{x}) \end{pmatrix}.$$

Assume that, for almost every (\mathbf{x}, λ) , the random vector $F(\mathbf{x}, \lambda)$ is nondegenerate⁵, that

$$\mathbb{P}(\det J_F(\mathbf{x}, \lambda) = 0 \mid F(\mathbf{x}, \lambda) = \mathbf{0}) = 0,$$

where $J_F(\mathbf{x}, \lambda)$ denotes the Jacobian matrix of F with respect to (\mathbf{x}, λ) , and that the integrand below is integrable on a region $U := U_{\mathbf{x}} \times U_{\lambda}$, with $U_{\lambda} \subset \mathbb{R} \setminus \{0\}$. Then

$$\mathbb{E} \left[\#\{(\mathbf{x}, \lambda) \in U : F(\mathbf{x}, \lambda) = \mathbf{0}\} \right] = \int_U |\lambda|^{-n} p_{(f(\mathbf{x}), \nabla f(\mathbf{x}))} \left(0, \frac{\xi - \mathbf{x}}{\lambda} \right) \mathcal{I}(\mathbf{x}, \lambda) d(\mathbf{x}, \lambda),$$

⁵By nondegenerate we mean that, for fixed (\mathbf{x}, λ) , the random vector $F(\mathbf{x}, \lambda)$ is not supported on any proper affine subspace of \mathbb{R}^{n+1} , equivalently that it admits a density with respect to Lebesgue measure on \mathbb{R}^{n+1} .

where $p_{(f(\mathbf{x}), \nabla f(\mathbf{x}))}$ is the joint density of $(f(\mathbf{x}), \nabla f(\mathbf{x}))$,

$$\mathcal{I}(\mathbf{x}, \lambda) = \mathbb{E} \left[\left| \nabla f(\mathbf{x})^\top \text{adj}(I_n + \lambda \nabla^2 f(\mathbf{x})) \nabla f(\mathbf{x}) \right| \middle| f(\mathbf{x}) = 0, \nabla f(\mathbf{x}) = \frac{\xi - \mathbf{x}}{\lambda} \right],$$

with $\text{adj}(\cdot)$ the adjugate of a square matrix.

Proof. Kac (1943) and Rice (1944) developed a formula to compute the expected number of zeros of a random field using the joint density of the field and its derivatives. A more contemporary treatment can be found in the work of Berzin et al. (2022).

Kac–Rice formula states that the expected number of zeros of a random field $F : \mathbb{R}^m \rightarrow \mathbb{R}^m$ in a Borel set $U \subseteq \mathbb{R}^m$ is given by

$$\mathbb{E} \left[\#\{\mathbf{z} \in U : F(\mathbf{z}) = 0\} \right] = \int_U \mathbb{E} [|\det J_F(\mathbf{z})| \mid F(\mathbf{z}) = 0] p_{F(\mathbf{z})}(0) d\mathbf{z},$$

where $J_F(\mathbf{z})$ is the Jacobian of F at \mathbf{z} , and $p_{F(\mathbf{z})}(0)$ is the density of $F(\mathbf{z})$ evaluated at zero. Apply this formula to the random field $F(\mathbf{x}, \lambda)$ defined in the proposition, we have

$$\mathbb{E} \left[\#\{(\mathbf{x}, \lambda) \in U : F(\mathbf{x}, \lambda) = 0\} \right] = \int_U \mathbb{E} [|\det J_F(\mathbf{x}, \lambda)| \mid F(\mathbf{x}, \lambda) = 0] p_{F(\mathbf{x}, \lambda)}(0) d\mathbf{x} d\lambda. \quad (7)$$

To find the $\det J_F(\mathbf{x}, \lambda)$, we compute the Jacobian matrix

$$J_F(\mathbf{x}, \lambda) = \begin{pmatrix} \nabla f(\mathbf{x})^\top & 0 \\ I_n + \lambda \nabla^2 f(\mathbf{x}) & \nabla f(\mathbf{x}) \end{pmatrix},$$

where $\nabla^2 f(\mathbf{x})$ is the Hessian matrix of f at \mathbf{x} . By the column swap rule of determinants, we have

$$\det J_F(\mathbf{x}, \lambda) = (-1)^n \det \begin{pmatrix} 0 & \nabla f(\mathbf{x})^\top \\ \nabla f(\mathbf{x}) & I_n + \lambda \nabla^2 f(\mathbf{x}) \end{pmatrix}.$$

Define the Schur complement of the block $I_n + \lambda \nabla^2 f(\mathbf{x})$ as

$$S(\mathbf{x}) := -\nabla f(\mathbf{x})^\top (I_n + \lambda \nabla^2 f(\mathbf{x}))^{-1} \nabla f(\mathbf{x}).$$

According to Schur's formula, we have

$$\det \begin{pmatrix} 0 & \nabla f(\mathbf{x})^\top \\ \nabla f(\mathbf{x}) & I_n + \lambda \nabla^2 f(\mathbf{x}) \end{pmatrix} = \det(I_n + \lambda \nabla^2 f(\mathbf{x})) \cdot \det(S(\mathbf{x})) = \det(I_n + \lambda \nabla^2 f(\mathbf{x})) \cdot S(\mathbf{x}).$$

The last equality holds since S is a scalar (1×1 matrix). Therefore,

$$\begin{aligned} |\det J_F(\mathbf{x}, \lambda)| &= \left| \det \begin{pmatrix} 0 & \nabla f(\mathbf{x})^\top \\ \nabla f(\mathbf{x}) & I_n + \lambda \nabla^2 f(\mathbf{x}) \end{pmatrix} \right| \\ &= |\det(I_n + \lambda \nabla^2 f(\mathbf{x})) \cdot S(\mathbf{x})| \\ &= |\det(I_n + \lambda \nabla^2 f(\mathbf{x})) \cdot \nabla f(\mathbf{x})^\top (I_n + \lambda \nabla^2 f(\mathbf{x}))^{-1} \nabla f(\mathbf{x})| \\ &= |\nabla f(\mathbf{x})^\top \text{adj}(I_n + \lambda \nabla^2 f(\mathbf{x})) \nabla f(\mathbf{x})|. \end{aligned}$$

On the other hand, since $F(\mathbf{x}, \lambda) = 0$ implies $f(\mathbf{x}) = 0$ and $\nabla f(\mathbf{x}) = (\xi - \mathbf{x})/\lambda$, by changing of variable, we have

$$p_{F(\mathbf{x}, \lambda)}(0) = p_{(f(\mathbf{x}), \nabla f(\mathbf{x}))}(0, \frac{\xi - \mathbf{x}}{\lambda}) \cdot |\det J_{\nabla f}(\mathbf{x})| = |\lambda|^{-n} p_{(f(\mathbf{x}), \nabla f(\mathbf{x}))}(0, \frac{\xi - \mathbf{x}}{\lambda}).$$

Combining the above results, we can obtain the desired formula for the expected number of real ED critical points. \square

B.6 Remark of Theorem 3.10

Remark B.1. When the random field is a Gaussian process, we provide some simplification of the above result. Let $f : \mathbb{R}^n \rightarrow \mathbb{R}$ be a Gaussian process, i.e., $f \sim \mathcal{GP}(0, K)$, with a covariance kernel $K_f : \mathbb{R}^n \times \mathbb{R}^n \rightarrow \mathbb{R}$ that is C^4 . Then the joint density term $p_{(f(\mathbf{x}), \nabla f(\mathbf{x}))}(0, \frac{\xi - \mathbf{x}}{\lambda})$ can be found by

$$p_{(f(\mathbf{x}), \nabla f(\mathbf{x}))}\left(0, \frac{\xi - \mathbf{x}}{\lambda}\right) = ((2\pi)^{n+1} K_f(\mathbf{x}, \mathbf{x}) \det S(\mathbf{x}))^{-\frac{1}{2}} \exp\left(-\frac{(\xi - \mathbf{x})^\top S(\mathbf{x})^{-1} (\xi - \mathbf{x})}{2\lambda^2}\right),$$

where $S(\mathbf{x}) \in \mathbb{R}^{n \times n}$ is defined as

$$S(\mathbf{x}) := \nabla_{\mathbf{x}} \nabla_{\mathbf{x}'}^\top K_f(\mathbf{x}, \mathbf{x}') \Big|_{\mathbf{x}'=\mathbf{x}} - \frac{\nabla_{\mathbf{x}} K_f(\mathbf{x}, \mathbf{x}') \Big|_{\mathbf{x}'=\mathbf{x}} (\nabla_{\mathbf{x}'} K_f(\mathbf{x}, \mathbf{x}') \Big|_{\mathbf{x}'=\mathbf{x}})^\top}{K_f(\mathbf{x}, \mathbf{x})}.$$

By Lemma B.2, the joint distribution of $(f(\mathbf{x}), \nabla f(\mathbf{x}))$ is Gaussian with mean zero and covariance

$$K_F(\mathbf{x}, \mathbf{x}) := \begin{bmatrix} K_f(\mathbf{x}, \mathbf{x}) & (\nabla_{\mathbf{x}'} K_f(\mathbf{x}, \mathbf{x}') \Big|_{\mathbf{x}'=\mathbf{x}})^\top \\ \nabla_{\mathbf{x}} K_f(\mathbf{x}, \mathbf{x}') \Big|_{\mathbf{x}'=\mathbf{x}} & \nabla_{\mathbf{x}} \nabla_{\mathbf{x}'}^\top K_f(\mathbf{x}, \mathbf{x}') \Big|_{\mathbf{x}'=\mathbf{x}} \end{bmatrix}.$$

Therefore, the density $p_{(f(\mathbf{x}), \nabla f(\mathbf{x}))}(0, \frac{\xi - \mathbf{x}}{\lambda})$ is given by

$$\begin{aligned} p_{(f(\mathbf{x}), \nabla f(\mathbf{x}))}(0, \frac{\xi - \mathbf{x}}{\lambda}) &= \frac{1}{(2\pi)^{(n+1)/2} \sqrt{\det K_F(\mathbf{x}, \mathbf{x})}} \exp\left(-\frac{1}{2} \begin{bmatrix} 0 \\ \frac{\xi - \mathbf{x}}{\lambda} \end{bmatrix}^\top K_F(\mathbf{x}, \mathbf{x})^{-1} \begin{bmatrix} 0 \\ \frac{\xi - \mathbf{x}}{\lambda} \end{bmatrix}\right) \\ &= \frac{1}{\sqrt{(2\pi)^{n+1} K_f(\mathbf{x}, \mathbf{x}) \det S(\mathbf{x})}} \exp\left(-\frac{(\xi - \mathbf{x})^\top S(\mathbf{x})^{-1} (\xi - \mathbf{x})}{2\lambda^2}\right), \end{aligned} \quad (8)$$

where the last equality follows from the block matrix inversion formula via Schur complement. To find $\mathcal{I}(\mathbf{x}, \lambda)$, we need to find the conditional distribution of $\nabla^2 f(\mathbf{x})$ given $f(\mathbf{x}) = 0$ and $\nabla f(\mathbf{x}) = \frac{\xi - \mathbf{x}}{\lambda}$. Since the kernel K_f is C^4 , by a similar argument as in Lemma B.2, the joint distribution of $(f(\mathbf{x}), \nabla f(\mathbf{x}), \text{vech}(\nabla^2 f(\mathbf{x})))$ is still Gaussian. The covariance matrix can be computed using the derivatives of the kernel K_f , i.e.,

$$\begin{aligned} \text{Cov}(\partial_{ij} f(\mathbf{x}), f(\mathbf{x})) &= \partial_{x_i} \partial_{x_j} K(\mathbf{x}, \mathbf{x}') \Big|_{\mathbf{x}'=\mathbf{x}}, \\ \text{Cov}(\partial_{ij} f(\mathbf{x}), \partial_k f(\mathbf{x})) &= \partial_{x_i} \partial_{x_j} \partial_{x'_k} K(\mathbf{x}, \mathbf{x}') \Big|_{\mathbf{x}'=\mathbf{x}}, \\ \text{Cov}(\partial_{ij} f(\mathbf{x}), \partial_{k\ell} f(\mathbf{x})) &= \partial_{x_i} \partial_{x_j} \partial_{x'_k} \partial_{x'_\ell} K(\mathbf{x}, \mathbf{x}') \Big|_{\mathbf{x}'=\mathbf{x}}. \end{aligned}$$

We don't provide the explicit formula here due to its complexity, but it can be derived using standard results on conditional distributions of multivariate Gaussians. Giving closed-form expressions for the expected number of real ED critical points would be challenging in general, but it may be possible for some specific kernels due to their special structures. For example, when K_f is a stationary kernel, i.e., $K_f(\mathbf{x}, \mathbf{x}') = \kappa(\mathbf{x} - \mathbf{x}')$ for some function $\kappa : \mathbb{R}^n \rightarrow \mathbb{R}$, $f(\mathbf{x})$ and $\nabla f(\mathbf{x})$ are independent random variables, which simplifies the expression of $p_{(f(\mathbf{x}), \nabla f(\mathbf{x}))}(0, \frac{\xi - \mathbf{x}}{\lambda})$ significantly.

Lemma B.2. Let $f : \mathbb{R}^n \rightarrow \mathbb{R}$ be a centered Gaussian process with kernel $K_f \in C^2$. Define the augmented process $g(\mathbf{x}) = \begin{bmatrix} f(\mathbf{x}) \\ \nabla f(\mathbf{x}) \end{bmatrix} \in \mathbb{R}^{n+1}$, where $\nabla f(\mathbf{x})$ is the gradient of f at \mathbf{x} . Then, $g : \mathbb{R}^n \rightarrow \mathbb{R}^{n+1}$ is a vector-valued Gaussian process with mean zero and kernel

$$K_g(\mathbf{x}, \mathbf{x}') = \begin{bmatrix} K_f(\mathbf{x}, \mathbf{x}') & (\nabla_{\mathbf{x}'} K_f(\mathbf{x}, \mathbf{x}'))^\top \\ \nabla_{\mathbf{x}} K_f(\mathbf{x}, \mathbf{x}') & \nabla_{\mathbf{x}} \nabla_{\mathbf{x}'}^\top K_f(\mathbf{x}, \mathbf{x}') \end{bmatrix}.$$

Proof. We first show that $g(\mathbf{x})$ is a Gaussian process. We need to show that, if we fix any finite set of points $\mathbf{x}^{(1)}, \dots, \mathbf{x}^{(m)} \in \mathbb{R}^n$, then any linear combination of the random variables $g(\mathbf{x}^{(1)}), \dots, g(\mathbf{x}^{(m)})$ is Gaussian. Let $\alpha^{(1)}, \dots, \alpha^{(m)} \in \mathbb{R}$ and $\beta^{(1)}, \dots, \beta^{(m)} \in \mathbb{R}^n$ be arbitrary. For each $i \in [m]$ and $j \in [n]$, define the difference quotient random variables

$$D_h^{(i,j)} := \frac{f(\mathbf{x}^{(i)} + h \mathbf{e}_j) - f(\mathbf{x}^{(i)})}{h}, \quad h \neq 0,$$

where \mathbf{e}_j is the j -th standard basis vector in \mathbb{R}^n . Since $(f(\mathbf{x}^{(i)} + h\mathbf{e}_j), f(\mathbf{x}^{(i)}))$ is jointly Gaussian, each $D_h^{(i,j)}$ is Gaussian, and hence any finite linear combination

$$S_h := \sum_{i=1}^m \alpha^{(i)} f(\mathbf{x}^{(i)}) + \sum_{i=1}^m \sum_{j=1}^n \beta_j^{(i)} D_h^{(i,j)}$$

is Gaussian for every fixed $h \neq 0$.

Because K_f is C^2 , the mean-square derivatives of f exist and coincide with the gradient components $\partial_j f(\mathbf{x}^{(i)})$, and moreover

$$D_h^{(i,j)} \xrightarrow[h \rightarrow 0]{} \partial_j f(\mathbf{x}^{(i)}) \quad \text{in } L^2.$$

Consequently, $S_h \rightarrow S$ in L^2 , where

$$S = \sum_{i=1}^m \alpha^{(i)} f(\mathbf{x}^{(i)}) + \sum_{i=1}^m \sum_{j=1}^n \beta_j^{(i)} \partial_j f(\mathbf{x}^{(i)}).$$

Since an L^2 -limit of Gaussian random variables is Gaussian, it follows that S is Gaussian. This proves that $(g(\mathbf{x}^{(1)}), \dots, g(\mathbf{x}^{(m)}))$ is jointly Gaussian, hence g is a vector-valued Gaussian process.

Next, we compute the mean and kernel of g . Since f is centered, we have $\mathbb{E}[\nabla f(\mathbf{x})] = \nabla_{\mathbf{x}} \mathbb{E}[f(\mathbf{x})] = 0$ due to the mean-square differentiability of f . Therefore, $\mathbb{E}[g(\mathbf{x})] = 0$.

It remains to compute the covariance blocks. We have $\text{Cov}(f(\mathbf{x}), f(\mathbf{x}')) = K_f(\mathbf{x}, \mathbf{x}')$ by definition. For the cross-covariance, using mean-square differentiability, we have

$$\text{Cov}(f(\mathbf{x}), \nabla f(\mathbf{x}')) = \mathbb{E}[f(\mathbf{x})(\nabla f(\mathbf{x}'))^\top] = \nabla_{\mathbf{x}'} \mathbb{E}[f(\mathbf{x}) f(\mathbf{x}')] = \nabla_{\mathbf{x}'} K_f(\mathbf{x}, \mathbf{x}').$$

which gives the top-right block as $(\nabla_{\mathbf{x}'} K_f(\mathbf{x}, \mathbf{x}'))^\top$. Similarly,

$$\text{Cov}(\nabla f(\mathbf{x}), f(\mathbf{x}')) = \nabla_{\mathbf{x}} K_f(\mathbf{x}, \mathbf{x}'),$$

and for the bottom-right block,

$$\text{Cov}(\nabla f(\mathbf{x}), \nabla f(\mathbf{x}')) = \mathbb{E}[\nabla_{\mathbf{x}} f(\mathbf{x})(\nabla_{\mathbf{x}'} f(\mathbf{x}'))^\top] = \nabla_{\mathbf{x}} \nabla_{\mathbf{x}'}^\top \mathbb{E}[f(\mathbf{x}) f(\mathbf{x}')] = \nabla_{\mathbf{x}} \nabla_{\mathbf{x}'}^\top K_f(\mathbf{x}, \mathbf{x}').$$

Stacking these blocks yields the stated matrix-valued kernel K_g . \square

B.7 Proof of Corollary 3.11

Corollary 3.11. *Let $f : \mathbb{R} \rightarrow \mathbb{R}$ be the neural network Gaussian process (NNGP) induced by an infinite-width two-layer network with polynomial activation of degree $d \geq 1$. Let $U = \mathbb{R} \times (\mathbb{R} \setminus \{0\})$. Then the expected real ED degree is*

$$\mathbb{E}[\#\{(x, \lambda) \in U : F(x, \lambda) = 0\}] = \frac{d}{\sqrt{2d-1}}.$$

Proof. When the input dimension of f is $n = 1$, the hypersurface $\{x \in \mathbb{R} : f(x) = 0\}$ degenerates to a finite set of points. In this case, the number of real ED critical points coincides with the number of real zeros of the random function $f(x) = 0$. By Proposition B.3, f is a centered Gaussian process with kernel $K(x, x')$ defined as

$$K(x, x') := \sum_{s=0}^{\lfloor \frac{d}{2} \rfloor} c(s, d) (x^2 + 1)^s ((x')^2 + 1)^s (xx' + 1)^{d-2s},$$

where $c(s, d) = \frac{(d!)^2}{2^{2s} (s!)^2 (d-2s)!}$. When $x' = x$, the kernel simplifies to

$$K(x, x) = \text{Var}[f(x)] = (2d-1)!! (x^2 + 1)^d.$$

According to Kac–Rice formula, the expected number of real zeros of f in an interval $U \subseteq \mathbb{R}$ is given by

$$\mathbb{E}[\#\{x \in U : f(x) = 0\}] = \int_U \mathbb{E}[|f'(x)| \mid f(x) = 0] p_{f(x)}(0) dx.$$

We define the Kac–Rice density as

$$\rho(x) := \mathbb{E} [|f'(x)| \mid f(x) = 0] p_{f(x)}(0).$$

Expressing the conditional expectation using the joint density of $(f(x), f'(x))$, we have

$$\begin{aligned} \rho(x) &= \int_{\mathbb{R}} |y| p_{(f(x), f'(x))}(0, y) dy \\ &= \int_{\mathbb{R}} |y| \frac{p_{(f(x), f'(x))}(0, y)}{p_{f(x)}(0)} p_{f(x)}(0) dy \\ &= \int_{\mathbb{R}} |y| p_{(f(x), f'(x))}(0, y) dy. \end{aligned}$$

The joint density $p_{(f(x), f'(x))}(0, y)$ is a bivariate Gaussian density with mean zero and covariance

$$K_F(x, x) := \begin{bmatrix} K(x, x) & \partial_{x'} K(x, x') \big|_{x'=x} \\ \partial_x K(x, x') \big|_{x'=x} & \partial_x \partial_{x'} K(x, x') \big|_{x'=x} \end{bmatrix}.$$

Then we have

$$\begin{aligned} \rho(x) &= \int_{\mathbb{R}} |y| \frac{1}{2\pi\sqrt{\det K_F(x, x)}} \exp\left(-\frac{1}{2} \begin{bmatrix} 0 \\ y \end{bmatrix}^\top K_F(x, x)^{-1} \begin{bmatrix} 0 \\ y \end{bmatrix}\right) dy \\ &= \int_{\mathbb{R}} |y| \frac{1}{2\pi\sqrt{\det K_F(x, x)}} \exp\left(-\frac{y^2}{2} \cdot \frac{K(x, x)}{\det K_F(x, x)}\right) dy \\ &= \frac{1}{2\pi\sqrt{\det K_F(x, x)}} \cdot \frac{2\det K_F(x, x)}{K(x, x)} \\ &= \frac{\sqrt{\det K_F(x, x)}}{\pi K(x, x)}. \end{aligned}$$

By Proposition B.5, we have

$$\begin{aligned} \partial_x K(x, x') \big|_{x'=x} &= d(2d-1)!! x (x^2 + 1)^{d-1}, \\ \partial_x \partial_{x'} K(x, x') \big|_{x'=x} &= 2d^2(d-1)(2d-3)!! x^2 (x^2 + 1)^{d-2} + d^2(2d-3)!! (x^2 + 1)^{d-1}. \end{aligned}$$

The determinant of $K_F(x, x)$ can be computed as

$$\begin{aligned} \det K_F(x, x) &= K(x, x) \cdot \partial_x \partial_{x'} K(x, x') \big|_{x'=x} - (\partial_{x'} K(x, x') \big|_{x'=x})^2 \\ &= (2d-1)!!(x^2 + 1)^d \cdot [2d^2(d-1)(2d-3)!! x^2 (x^2 + 1)^{d-2} + d^2(2d-3)!! (x^2 + 1)^{d-1}] \\ &\quad - [d(2d-1)!! x (x^2 + 1)^{d-1}]^2 \\ &= d^2(2d-1)((2d-3)!!)^2 (x^2 + 1)^{2d-2}. \end{aligned}$$

The Kac–Rice density can then be found by

$$\rho(x) = \frac{\sqrt{\det K_F(x, x)}}{\pi K(x, x)} = \frac{d\sqrt{(2d-1)(2d-3)!!}(x^2 + 1)^{d-1}}{\pi(2d-1)!!(x^2 + 1)^d} = \frac{d}{\sqrt{2d-1}} \cdot \frac{1}{\pi(x^2 + 1)}.$$

Therefore, the expected number of real zeros of f in an \mathbb{R} is given by

$$\mathbb{E} [\#\{x \in U : f(x) = 0\}] = \int_{\mathbb{R}} \rho(x) dx = \int_{\mathbb{R}} \frac{d}{\sqrt{2d-1}} \cdot \frac{1}{\pi(x^2 + 1)} dx = \frac{d}{\sqrt{2d-1}}.$$

Figure 5 shows a simulation study that verifies the above theoretical result. \square

Proposition B.3 (NNGP of shallow polynomial networks). *Consider a two-layer network of width m with element-wise polynomial activation $\sigma : \mathbb{R} \rightarrow \mathbb{R}$ given by $\sigma(z) = z^d$ for some integer $d \geq 1$. For an input $\mathbf{x} \in \mathbb{R}^n$, the network output $f_m : \mathbb{R}^n \rightarrow \mathbb{R}$ is*

$$f_m(\mathbf{x}) = \frac{1}{\sqrt{m}} \sum_{i=1}^m a_i \sigma(\mathbf{w}_i^\top \mathbf{x} + b_i) = \frac{1}{\sqrt{m}} \sum_{i=1}^m a_i (\mathbf{w}_i^\top \mathbf{x} + b_i)^d,$$

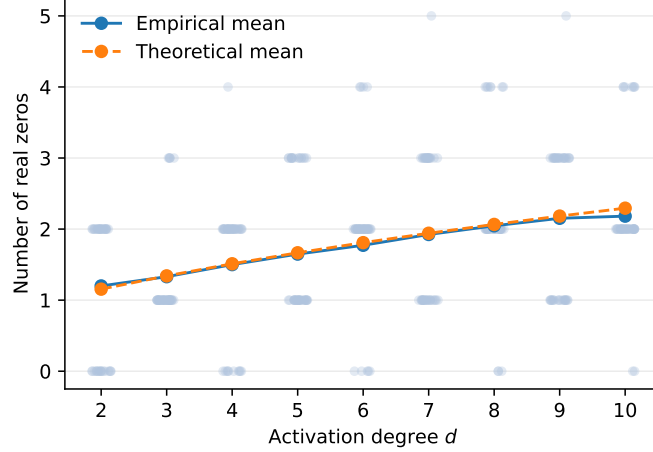


Figure 5: Number of real zeros vs. activation degree. Light points show individual simulations; solid and dashed lines denote empirical and theoretical means ($n = 1,000$ samples, $m = 20,000$ hidden units).

where $\mathbf{w}_i \in \mathbb{R}^n$ and b_i are the hidden-layer weights and biases, respectively, and $a_i \in \mathbb{R}$ are the output-layer weights. Let the parameters $\{a_i, \mathbf{w}_i, b_i\}_{i=1}^m$ be initialized i.i.d. from

$$a_i \sim \mathcal{N}(0, 1), \quad b_i \sim \mathcal{N}(0, 1), \quad \mathbf{w}_i \sim \mathcal{N}(0, \frac{1}{n} I_n).$$

Then, as $m \rightarrow \infty$, the network output converges in distribution to a Gaussian process

$$f(\mathbf{x}) \sim \mathcal{GP}(0, K),$$

where the kernel function is given by

$$K(\mathbf{x}, \mathbf{x}') := \sum_{s=0}^{\lfloor \frac{d}{2} \rfloor} c(s, d) \left(\frac{1}{n} \|\mathbf{x}\|_2^2 + 1 \right)^s \left(\frac{1}{n} \|\mathbf{x}'\|_2^2 + 1 \right)^s \left(\frac{1}{n} \mathbf{x}^\top \mathbf{x}' + 1 \right)^{d-2s}, \quad (9)$$

with $c(s, d) = \frac{(d!)^2}{2^{2s} (s!)^2 (d - 2s)!}$. When $\mathbf{x} = \mathbf{x}'$, the kernel simplifies to

$$K(\mathbf{x}, \mathbf{x}) = \text{Var}[f(\mathbf{x})] = (2d - 1)!! \left(\frac{1}{n} \|\mathbf{x}\|_2^2 + 1 \right)^d.$$

Proof. For fixed \mathbf{x} , by the central limit theorem (CLT), as $m \rightarrow \infty$,

$$f_m(\mathbf{x}) \xrightarrow{d} \mathcal{N}(0, \mathbb{E}_{a, \mathbf{w}, b} [a^2 (\mathbf{w}^\top \mathbf{x} + b)^{2d}]).$$

Since a , \mathbf{w} , and b are independent, we have

$$\mathbb{E}_{a, \mathbf{w}, b} [a^2 (\mathbf{w}^\top \mathbf{x} + b)^{2d}] = \mathbb{E}_a [a^2] \cdot \mathbb{E}_{\mathbf{w}, b} [(\mathbf{w}^\top \mathbf{x} + b)^{2d}] = \mathbb{E}_{\mathbf{w}, b} [(\mathbf{w}^\top \mathbf{x} + b)^{2d}].$$

Next, we compute $\mathbb{E}_{\mathbf{w}, b} [(\mathbf{w}^\top \mathbf{x} + b)^{2d}]$. Note that $\mathbf{w}^\top \mathbf{x} + b$ is a Gaussian random variable with mean zero and variance $\frac{1}{n} \|\mathbf{x}\|_2^2 + 1$. Therefore, using the moment formula for Gaussian random variables, we have

$$\mathbb{E}_{\mathbf{w}, b} [(\mathbf{w}^\top \mathbf{x} + b)^{2d}] = (2d - 1)!! \left(\frac{1}{n} \|\mathbf{x}\|_2^2 + 1 \right)^d.$$

Thus, the variance of $f(\mathbf{x})$ is

$$\text{Var}[f(\mathbf{x})] = (2d - 1)!! \left(\frac{1}{n} \|\mathbf{x}\|_2^2 + 1 \right)^d.$$

The kernel function $K(\mathbf{x}, \mathbf{x}')$ is given by

$$K(\mathbf{x}, \mathbf{x}') = \text{Cov}(f(\mathbf{x}), f(\mathbf{x}')) = \mathbb{E}_{a, \mathbf{w}, b}[a^2(\mathbf{w}^\top \mathbf{x} + b)^d(\mathbf{w}^\top \mathbf{x}' + b)^d] = \mathbb{E}_{\mathbf{w}, b}[(\mathbf{w}^\top \mathbf{x} + b)^d(\mathbf{w}^\top \mathbf{x}' + b)^d].$$

Recall Isserlis' theorem (Isserlis, 1918; Janson, 1997), which states that for zero-mean Gaussian random variables X_1, X_2, \dots, X_n ,

$$\mathbb{E}[X_1 X_2 \cdots X_n] = \sum_{p \in P_n^2} \prod_{\{i, j\} \in p} \mathbb{E}[X_i X_j],$$

where P_n^2 is the set of all pairwise partitions of $\{1, 2, \dots, n\}$. If (X, Y) is a bivariate zero-mean Gaussian vector, to find $\mathbb{E}[X^d Y^d]$, we consider all pairwise partitions of the multiset

$$\underbrace{\{X, X, \dots, X\}}_{d \text{ times}}, \quad \underbrace{\{Y, Y, \dots, Y\}}_{d \text{ times}}.$$

The partition that contributes to $\mathbb{E}[X^d Y^d]$ must pair each X with either another X or a Y , and similarly for each Y . Let s be the number of pairs of the form (X, X) (or equivalently (Y, Y)) in the partition. Then there are $d - 2s$ pairs of the form (X, Y) . The number of such partitions is

$$\binom{d}{d-2s}^2 (d-2s)! ((2s-1)!!)^2,$$

where $\binom{d}{d-2s}^2$ chooses which X 's and Y 's are paired together, $(d-2s)!$ counts the number of ways to pair the selected X 's with Y 's, and $((2s-1)!!)^2$ counts the number of ways to pair the remaining X 's and Y 's among themselves. Therefore, by Isserlis' theorem, we have

$$\begin{aligned} \mathbb{E}[X^d Y^d] &= \sum_{s=0}^{\lfloor \frac{d}{2} \rfloor} \binom{d}{d-2s}^2 (d-2s)! ((2s-1)!!)^2 \mathbb{E}[X^2]^s \mathbb{E}[Y^2]^s \mathbb{E}[XY]^{d-2s} \\ &= \sum_{s=0}^{\lfloor \frac{d}{2} \rfloor} \frac{(d!)^2}{((d-2s)!)^2 ((2s)!)^2} \cdot (d-2s)! \cdot \frac{((2s)!)^2}{2^{2s} (s!)^2} \mathbb{E}[X^2]^s \mathbb{E}[Y^2]^s \mathbb{E}[XY]^{d-2s} \\ &= \sum_{s=0}^{\lfloor \frac{d}{2} \rfloor} \frac{(d!)^2}{2^{2s} (s!)^2 (d-2s)!} \mathbb{E}[X^2]^s \mathbb{E}[Y^2]^s \mathbb{E}[XY]^{d-2s}. \end{aligned}$$

Let $X = \mathbf{w}^\top \mathbf{x} + b$ and $Y = \mathbf{w}^\top \mathbf{x}' + b$. Then, $\mathbb{E}[X^2] = \frac{1}{n} \|\mathbf{x}\|_2^2 + 1$, $\mathbb{E}[Y^2] = \frac{1}{n} \|\mathbf{x}'\|_2^2 + 1$, and $\mathbb{E}[XY] = \frac{1}{n} \mathbf{x}^\top \mathbf{x}' + 1$. Substituting these into the expression for $\mathbb{E}[X^d Y^d]$ yields the desired kernel formula. \square

Remark B.4. We provide two identities about the coefficients $c(s, d)$ appearing in Equation (9). These identities can be useful in simplifying certain expressions involving the kernel.

$$\sum_{s=0}^{\lfloor \frac{d}{2} \rfloor} c_{s,d} = (2d-1)!! \tag{10}$$

$$\sum_{s=0}^{\lfloor \frac{d}{2} \rfloor} c_{s,d} \cdot s = \frac{d(d-1)(2d-3)!!}{2} \tag{11}$$

The first identity follows from the expression of $K_f(\mathbf{x}, \mathbf{x})$. To show the second identity, we note that

$$\frac{c_{s,d}}{c_{s,d-1}} = \frac{d^2}{d-2s}.$$

Therefore, we have

$$\sum_{s=0}^{\lfloor \frac{d}{2} \rfloor} c_{s,d} \cdot (d-2s) = d^2 \sum_{s=0}^{\lfloor \frac{d-1}{2} \rfloor} c_{s,d-1}.$$

Re-arranging the above equation gives

$$\sum_{s=0}^{\lfloor \frac{d}{2} \rfloor} c_{s,d} \cdot s = \frac{d}{2} \left(\sum_{s=0}^{\lfloor \frac{d}{2} \rfloor} c_{s,d} - d \sum_{s=0}^{\lfloor \frac{d-1}{2} \rfloor} c_{s,d-1} \right) = \frac{d}{2} ((2d-1)!! - d(2d-3)!!) = \frac{d(d-1)(2d-3)!!}{2}.$$

Proposition B.5. Given the kernel function $K : \mathbb{R}^n \times \mathbb{R}^n \rightarrow \mathbb{R}$ defined as in Equation (9), its first and second derivatives evaluated at the same point $\mathbf{x}' = \mathbf{x}$ are given by

$$\begin{aligned}\nabla_{\mathbf{x}} K(\mathbf{x}, \mathbf{x}')|_{\mathbf{x}'=\mathbf{x}} &= \frac{d(2d-1)!!}{n} \left(\frac{1}{n} \|\mathbf{x}\|_2^2 + 1 \right)^{d-1} \mathbf{x} \\ \nabla_{\mathbf{x}} \nabla_{\mathbf{x}'}^\top K(\mathbf{x}, \mathbf{x}')|_{\mathbf{x}'=\mathbf{x}} &= \frac{2d^2(d-1)(2d-3)!!}{n^2} \left(\frac{1}{n} \|\mathbf{x}\|_2^2 + 1 \right)^{d-2} \cdot \mathbf{x} \mathbf{x}^\top \\ &\quad + \frac{d^2(2d-3)!!}{n} \left(\frac{1}{n} \|\mathbf{x}\|_2^2 + 1 \right)^{d-1} \cdot I_n.\end{aligned}$$

Proof. To compute the gradient block $\nabla_{\mathbf{x}} K(\mathbf{x}, \mathbf{x}')|_{\mathbf{x}'=\mathbf{x}}$, we first compute the total derivative of $K(\mathbf{x}, \mathbf{x})$ with respect to \mathbf{x} . By the chain rule and symmetry of the kernel, we have

$$\frac{d K(\mathbf{x}, \mathbf{x})}{d \mathbf{x}} = (\nabla_{\mathbf{x}} K(\mathbf{x}, \mathbf{x}') + \nabla_{\mathbf{x}'} K(\mathbf{x}, \mathbf{x}'))|_{\mathbf{x}'=\mathbf{x}} = 2 \cdot \nabla_{\mathbf{x}} K(\mathbf{x}, \mathbf{x}')|_{\mathbf{x}'=\mathbf{x}}.$$

Therefore, we have

$$\nabla_{\mathbf{x}} K(\mathbf{x}, \mathbf{x}')|_{\mathbf{x}'=\mathbf{x}} = \frac{1}{2} \cdot \frac{d K(\mathbf{x}, \mathbf{x})}{d \mathbf{x}} = \frac{d(2d-1)!!}{n} \left(\frac{1}{n} \|\mathbf{x}\|_2^2 + 1 \right)^{d-1} \mathbf{x}.$$

Next, we compute the Hessian block $\nabla_{\mathbf{x}} \nabla_{\mathbf{x}'}^\top K(\mathbf{x}, \mathbf{x}')|_{\mathbf{x}'=\mathbf{x}}$. $\nabla_{\mathbf{x}} K_f(\mathbf{x}, \mathbf{x}')$ can be computed as

$$\begin{aligned}\nabla_{\mathbf{x}} K_f(\mathbf{x}, \mathbf{x}') &= \sum_{s=0}^{\lfloor \frac{d}{2} \rfloor} c_{s,d} \left(\frac{1}{n} \|\mathbf{x}'\|_2^2 + 1 \right)^s \left(\frac{2s}{n} \left(\frac{1}{n} \|\mathbf{x}\|_2^2 + 1 \right)^{s-1} \left(\frac{1}{n} \mathbf{x}^\top \mathbf{x}' + 1 \right)^{d-2s} \mathbf{x} \right. \\ &\quad \left. + \frac{d-2s}{n} \left(\frac{1}{n} \|\mathbf{x}\|_2^2 + 1 \right)^s \left(\frac{1}{n} \mathbf{x}^\top \mathbf{x}' + 1 \right)^{d-2s-1} \mathbf{x}' \right) \\ &= \sum_{s=0}^{\lfloor \frac{d}{2} \rfloor} c_{s,d} \left(\frac{1}{n} \|\mathbf{x}'\|_2^2 + 1 \right)^s \left(\frac{1}{n} \|\mathbf{x}\|_2^2 + 1 \right)^{s-1} \left(\frac{1}{n} \mathbf{x}^\top \mathbf{x}' + 1 \right)^{d-2s-1} \\ &\quad \cdot \left(\frac{2s}{n} \left(\frac{1}{n} \mathbf{x}^\top \mathbf{x}' + 1 \right) \mathbf{x} + \frac{d-2s}{n} \left(\frac{1}{n} \|\mathbf{x}\|_2^2 + 1 \right) \mathbf{x}' \right).\end{aligned}$$

Furthermore, we can compute $\nabla_{\mathbf{x}} \nabla_{\mathbf{x}'}^\top K_f(\mathbf{x}, \mathbf{x}')$ by differentiating $\nabla_{\mathbf{x}} K_f(\mathbf{x}, \mathbf{x}')$ with respect to \mathbf{x}' . Applying the product rule and chain rule, we obtain

$$\begin{aligned}\nabla_{\mathbf{x}} \nabla_{\mathbf{x}'}^\top K_f(\mathbf{x}, \mathbf{x}') &= \sum_{s=0}^{\lfloor \frac{d}{2} \rfloor} c_{s,d} \left(\frac{1}{n} \|\mathbf{x}\|_2^2 + 1 \right)^{s-1} \left(\frac{1}{n} \|\mathbf{x}'\|_2^2 + 1 \right)^{s-1} \left(\frac{1}{n} \mathbf{x}^\top \mathbf{x}' + 1 \right)^{d-2s-2} \\ &\quad \cdot \left[\frac{2s}{n} \left(\frac{1}{n} \mathbf{x}^\top \mathbf{x}' + 1 \right) \left(\frac{2s}{n} \left(\frac{1}{n} \mathbf{x}^\top \mathbf{x}' + 1 \right) \mathbf{x} + \frac{d-2s}{n} \left(\frac{1}{n} \|\mathbf{x}\|_2^2 + 1 \right) \mathbf{x}' \right) \mathbf{x}'^\top \right. \\ &\quad \left. + \frac{d-2s-1}{n} \left(\frac{1}{n} \|\mathbf{x}'\|_2^2 + 1 \right) \left(\frac{2s}{n} \left(\frac{1}{n} \mathbf{x}^\top \mathbf{x}' + 1 \right) \mathbf{x} + \frac{d-2s}{n} \left(\frac{1}{n} \|\mathbf{x}\|_2^2 + 1 \right) \mathbf{x}' \right) \mathbf{x}^\top \right. \\ &\quad \left. + \left(\frac{1}{n} \mathbf{x}^\top \mathbf{x}' + 1 \right) \left(\frac{1}{n} \|\mathbf{x}'\|_2^2 + 1 \right) \left(\frac{2s}{n} \cdot \frac{1}{n} \cdot \mathbf{x} \mathbf{x}'^\top + \frac{d-2s}{n} \left(\frac{1}{n} \|\mathbf{x}'\|_2^2 + 1 \right) \cdot I_n \right) \right].\end{aligned}$$

Evaluating the above expression at $\mathbf{x}' = \mathbf{x}$ and simplifying using the identities for $c_{s,d}$ yields

$$\begin{aligned}\nabla_{\mathbf{x}} \nabla_{\mathbf{x}'}^\top K_f(\mathbf{x}, \mathbf{x}')|_{\mathbf{x}'=\mathbf{x}} &= \sum_{s=0}^{\lfloor \frac{d}{2} \rfloor} c_{s,d} \left(\frac{d(d-1) + 2s}{n^2} \cdot \left(\frac{1}{n} \|\mathbf{x}\|_2^2 + 1 \right)^{d-2} \cdot \mathbf{x} \mathbf{x}^\top + \frac{d-2s}{n} \cdot \left(\frac{1}{n} \|\mathbf{x}\|_2^2 + 1 \right)^{d-1} \cdot I_n \right) \\ &= \frac{2d^2(d-1)(2d-3)!!}{n^2} \left(\frac{1}{n} \|\mathbf{x}\|_2^2 + 1 \right)^{d-2} \cdot \mathbf{x} \mathbf{x}^\top + \frac{d^2(2d-3)!!}{n} \left(\frac{1}{n} \|\mathbf{x}\|_2^2 + 1 \right)^{d-1} \cdot I_n. \quad (12)\end{aligned}$$

□

B.8 Proof of Proposition 4.5

Proposition 4.5. *Let $\mathcal{V} = \{\mathbf{x} : \ell_1(\mathbf{x})\ell_2(\mathbf{x}) = 0\}$ be a reducible quadratic hypersurface consisting of two non-parallel hyperplanes. The ED degree of \mathcal{V} is 2. The two critical points collide if and only if the data \mathbf{u} lies on the intersection of the two hyperplanes $\ell_1(\mathbf{u}) = \ell_2(\mathbf{u}) = 0$. Consequently, the ED discriminant is contained in the model \mathcal{V} .*

Proof. The hypersurface \mathcal{V} is the union of two hyperplanes $H_1 = \{\mathbf{x} : \ell_1(\mathbf{x}) = 0\}$ and $H_2 = \{\mathbf{x} : \ell_2(\mathbf{x}) = 0\}$. For a generic data point \mathbf{u} , the ED critical points on \mathcal{V} are simply the orthogonal projections of \mathbf{u} onto H_1 and H_2 . Let these projections be $p_1(\mathbf{u})$ and $p_2(\mathbf{u})$. Thus, there are exactly two critical points. These two solutions collide precisely when $p_1(\mathbf{u}) = p_2(\mathbf{u})$. Let this common point be \mathbf{x}^* . Since $\mathbf{x}^* \in H_1$ and $\mathbf{x}^* \in H_2$, it must lie in the intersection $H_1 \cap H_2$. The condition that \mathbf{x}^* is the orthogonal projection of \mathbf{u} onto H_1 implies that the vector $\mathbf{u} - \mathbf{x}^*$ is normal to H_1 . Similarly, $\mathbf{u} - \mathbf{x}^*$ must be normal to H_2 .

Since the normals of H_1 and H_2 are not parallel by assumption, the only vector simultaneously normal to two transverse hyperplanes is the zero vector. Therefore, we must have $\mathbf{u} - \mathbf{x}^* = \mathbf{0}$, which implies $\mathbf{u} = \mathbf{x}^*$. Thus, the critical points coincide if and only if $\mathbf{u} \in H_1 \cap H_2 \subseteq \mathcal{V}$. □

B.9 Proof of Theorem 4.6

Theorem 4.6. *The ED degree of the decision boundary $\text{EDdegree}(\mathcal{V}_{c,c'}^\theta)$ is given by*

$$\begin{cases} 2r & \text{if } \text{rank}(M_\theta) = \text{rank}(A_\theta) + 1 \\ 2r + 1 & \text{if } \text{rank}(M_\theta) = \text{rank}(A_\theta) + 2 \\ 2r - 2 & \text{if } \text{rank}(M_\theta) = \text{rank}(A_\theta). \end{cases}$$

Proof. The ED degree of $\mathcal{V}_{c,c'}^\theta$ is the number of complex critical points of the squared distance function $d_{\mathbf{u}}(\mathbf{x})$ restricted to the regular part $(\mathcal{V}_{c,c'}^\theta)_{\text{reg}}$ for a generic data point $\mathbf{u} \in \mathbb{C}^n$. The critical points satisfy the Lagrange multiplier condition, which states that the vector $\mathbf{u} - \mathbf{x}$ is normal to the tangent space of $\mathcal{V}_{c,c'}^\theta$ at \mathbf{x} . Algebraically, this implies $\mathbf{u} - \mathbf{x} = \lambda \nabla B_\theta(\mathbf{x})$ for some scalar $\lambda \in \mathbb{C}^*$. Substituting the gradient $\nabla B_\theta(\mathbf{x}) = 2A_\theta \mathbf{x} + \mathbf{b}_\theta$, we obtain the system:

$$\mathbf{u} - \mathbf{x} = \lambda(2A_\theta \mathbf{x} + \mathbf{b}_\theta).$$

Rearranging terms yields a linear system for \mathbf{x} parameterized by λ :

$$(I + 2\lambda A_\theta) \mathbf{x} = \mathbf{u} - \lambda \mathbf{b}_\theta. \quad (13)$$

For a generic \mathbf{u} , the matrix $(I + 2\lambda A_\theta)$ is invertible for all solutions λ . We solve for \mathbf{x} by changing the coordinate system (rotating) to the eigenbasis of A_θ .

Since A_θ is symmetric, it is orthogonally diagonalizable over \mathbb{R} . Let $A_\theta = U \Sigma U^\top$ be its spectral decomposition, where U is an orthogonal matrix ($U^\top U = I$) and $\Sigma = \text{diag}(\sigma_1, \dots, \sigma_n)$ contains the eigenvalues. We rotate the coordinate system to the eigenbasis of A_θ by defining

$$\tilde{\mathbf{x}} = U^\top \mathbf{x}, \quad \tilde{\mathbf{u}} = U^\top \mathbf{u}, \quad \tilde{\mathbf{b}} = U^\top \mathbf{b}_\theta.$$

In these coordinates A_θ is diagonal, and the linear system decouples into scalar equations for each component $i \in [n]$:

$$(1 + 2\lambda\sigma_i)\tilde{x}_i = \tilde{u}_i - \lambda\tilde{b}_i \implies \tilde{x}_i(\lambda) = \frac{\tilde{u}_i - \lambda\tilde{b}_i}{1 + 2\lambda\sigma_i}.$$

Substituting these parameterized coordinates back into the defining equation $B_\theta(\mathbf{x}) = \tilde{\mathbf{x}}^\top \Sigma \tilde{\mathbf{x}} + \tilde{\mathbf{b}}^\top \tilde{\mathbf{x}} + c_\theta = 0$ yields a univariate rational equation in λ , which we denote by $E(\lambda) = 0$:

$$E(\lambda) := \sum_{i=1}^n \sigma_i \left(\frac{\tilde{u}_i - \lambda\tilde{b}_i}{1 + 2\lambda\sigma_i} \right)^2 + \sum_{i=1}^n \tilde{b}_i \left(\frac{\tilde{u}_i - \lambda\tilde{b}_i}{1 + 2\lambda\sigma_i} \right) + c_\theta = 0. \quad (14)$$

Let r be the number of distinct non-zero eigenvalues of A_{θ} , denoted μ_1, \dots, μ_r . The common denominator of $E(\lambda)$ is $D(\lambda) = \prod_{j=1}^r (1 + 2\lambda\mu_j)^2$, which has degree $2r$. The ED degree of $\mathcal{V}_{c,c'}^{\theta}$ is given by the degree of the polynomial $P(\lambda)$, which is obtained from $E(\lambda)$ by clearing the denominators:

$$P(\lambda) = E(\lambda) \cdot D(\lambda).$$

Note that for generic \mathbf{u} , the correspondence between roots λ and critical points \mathbf{x} is bijective, as $D(\lambda)$ does not vanish at the roots of $P(\lambda)$ and the linear system uniquely determines \mathbf{x} .

To determine $\deg(P)$, we analyze the behavior of the rational function at infinity. Since $E(\lambda) = P(\lambda)/D(\lambda)$, the function scales as $E(\lambda) \sim \lambda^{\deg(P) - \deg(D)}$ as $\lambda \rightarrow \infty$. Letting $\text{ord}_{\infty}(E)$ denote this exponent of growth or decay, we obtain the relation:

$$\deg(P) - \deg(D) = \text{ord}_{\infty}(E) \implies \text{EDdegree}(\mathcal{V}_{c,c'}^{\theta}) = 2r + \text{ord}_{\infty}(E).$$

To determine the asymptotic behavior of $E(\lambda)$, we analyze the rank of the augmented matrix M_{θ} associated with the quadric. We partition the indices $\{1, \dots, n\}$ into two sets: $I_{\text{range}} = \{i \mid \sigma_i \neq 0\}$ and $I_{\text{ker}} = \{i \mid \sigma_i = 0\}$. The augmented matrix is given by:

$$M_{\theta} = \begin{pmatrix} A_{\theta} & \frac{1}{2}\mathbf{b}_{\theta} \\ \frac{1}{2}\mathbf{b}_{\theta}^{\top} & c_{\theta} \end{pmatrix}.$$

First, we apply the orthogonal change of basis U that diagonalizes A_{θ} . Second, we permute the coordinates to group the indices into the two sets I_{range} and I_{ker} . This transformation yields the partitioned matrix:

$$M'_{\theta} = \begin{pmatrix} \Sigma_{\text{range}} & 0 & \frac{1}{2}\tilde{\mathbf{b}}_{\text{range}} \\ 0 & 0 & \frac{1}{2}\tilde{\mathbf{b}}_{\text{ker}} \\ \frac{1}{2}\tilde{\mathbf{b}}_{\text{range}}^{\top} & \frac{1}{2}\tilde{\mathbf{b}}_{\text{ker}}^{\top} & c_{\theta} \end{pmatrix}.$$

We perform symmetric block Gaussian elimination to eliminate the couplings between the range components and the affine part. Specifically, we subtract the projection of the first block-row onto the last row using the invertible pivot Σ_{range} . This operation zeroes out $\frac{1}{2}\tilde{\mathbf{b}}_{\text{range}}$ and transforms the constant c_{θ} into the Schur complement S :

$$S = c_{\theta} - \left(\frac{1}{2}\tilde{\mathbf{b}}_{\text{range}}^{\top}\right)\Sigma_{\text{range}}^{-1}\left(\frac{1}{2}\tilde{\mathbf{b}}_{\text{range}}\right) = c_{\theta} - \sum_{j \in I_{\text{range}}} \frac{\tilde{b}_j^2}{4\sigma_j}.$$

The resulting matrix is block-diagonal, decoupling the range variables from the kernel and constant terms:

$$M_{\theta} \cong \begin{pmatrix} \Sigma_{\text{range}} & 0 & 0 \\ 0 & 0 & \frac{1}{2}\tilde{\mathbf{b}}_{\text{ker}} \\ 0 & \frac{1}{2}\tilde{\mathbf{b}}_{\text{ker}}^{\top} & S \end{pmatrix}.$$

The rank of M_{θ} is the sum of $\text{rank}(\Sigma_{\text{range}}) = \text{rank } A_{\theta}$ and the rank of the residual block $K = \begin{pmatrix} 0 & \tilde{\mathbf{b}}_{\text{ker}}/2 \\ \tilde{\mathbf{b}}_{\text{ker}}^{\top}/2 & S \end{pmatrix}$.

We now analyze the cases.

Case 1: $\text{rank } M_{\theta} = \text{rank } A_{\theta} + 1$.

Since $\text{rank } M_{\theta} = \text{rank } A_{\theta} + \text{rank } K$, this condition implies that $\text{rank } K = 1$. This, in turn, forces $\tilde{\mathbf{b}}_{\text{ker}}$ to be zero. Indeed, if $\tilde{\mathbf{b}}_{\text{ker}}$ were not zero, we could pick a non-zero component $(\tilde{\mathbf{b}}_{\text{ker}})_i$. The 2×2 submatrix formed by this component and S would have determinant $-(\tilde{\mathbf{b}}_{\text{ker}})_i^2/4 \neq 0$, implying $\text{rank}(K) \geq 2$. This contradicts our assumption. Therefore, $\tilde{\mathbf{b}}_{\text{ker}} = 0$. With $\tilde{\mathbf{b}}_{\text{ker}} = 0$, the matrix becomes diagonal $K = \text{diag}(0, \dots, 0, S)$. Its rank is 1 if and only if $S \neq 0$.

We use these facts to find the degree of $E(\lambda)$. The terms in the sum (14) behave differently depending on whether the eigenvalue σ_i is zero or not. We formally split the sum into two parts:

$$E(\lambda) = E_{\text{range}}(\lambda) + E_{\text{ker}}(\lambda) + c_{\theta},$$

where E_{range} sums over indices with $\sigma_i \neq 0$, and E_{ker} sums over indices with $\sigma_i = 0$:

$$E_{\text{range}}(\lambda) := \sum_{i \in I_{\text{range}}} \left[\sigma_i \left(\frac{\tilde{u}_i - \lambda \tilde{b}_i}{1 + 2\lambda\sigma_i} \right)^2 + \tilde{b}_i \left(\frac{\tilde{u}_i - \lambda \tilde{b}_i}{1 + 2\lambda\sigma_i} \right) \right],$$

$$E_{\text{ker}}(\lambda) := \sum_{i \in I_{\text{ker}}} \tilde{b}_i (\tilde{u}_i - \lambda \tilde{b}_i).$$

Since $\tilde{b}_{\text{ker}} = 0$, the coefficients in the kernel sum are all zero, so $E_{\text{ker}}(\lambda) = 0$. We just need the limit of the remaining parts as $\lambda \rightarrow \infty$:

$$\lim_{\lambda \rightarrow \infty} E(\lambda) = \lim_{\lambda \rightarrow \infty} (E_{\text{range}}(\lambda) + c_{\theta}) = c_{\theta} - \sum_{j \in I_{\text{range}}} \frac{\tilde{b}_j^2}{4\sigma_j} = S.$$

Because $S \neq 0$, $E(\lambda)$ approaches a non-zero constant. This means the numerator polynomial $P(\lambda)$ has the same degree as the denominator $D(\lambda)$:

$$\text{EDdegree}(\mathcal{V}_{c,c'}^{\theta}) = \deg(D) = 2r.$$

Case 2: $\text{rank } M_{\theta} = \text{rank } A_{\theta} + 2$.

In this case, we get that $\text{rank } K = 2$. This implies $\tilde{b}_{\text{ker}} \neq 0$, as vanishing kernel components would restrict the rank of K to at most 1. We analyze the behavior of $E(\lambda) = E_{\text{range}}(\lambda) + E_{\text{ker}}(\lambda) + c_{\theta}$ as $\lambda \rightarrow \infty$. While the range terms converge to a constant, the non-zero kernel vector grows linearly:

$$E(\lambda) = -\lambda \sum_{j \in I_{\text{ker}}} \tilde{b}_j^2 + O(1).$$

Since the coefficient $-\sum \tilde{b}_j^2 = -\|\tilde{b}_{\text{ker}}\|^2$ is non-zero, this linear term dominates the behavior at infinity, implying $\text{ord}_{\infty}(E) = 1$. Thus, the degree of the numerator is one higher than the denominator:

$$\text{EDdegree}(\mathcal{V}_{c,c'}^{\theta}) = \deg(D) + 1 = 2r + 1.$$

Case 3: $\text{rank } M_{\theta} = \text{rank } A_{\theta}$.

The condition $\text{rank } M_{\theta} = \text{rank } A_{\theta} + \text{rank } K$ implies that the residual block K must be the zero matrix. This forces both $\tilde{b}_{\text{ker}} = 0$ and $S = 0$. We analyze the asymptotic behavior of the range terms $E(\lambda) = c_{\theta} + \sum_{i \in I_{\text{range}}} Q_i(T_i(\lambda))$, where $Q_i(t) = \sigma_i t^2 + \tilde{b}_i t$ and $T_i(\lambda) = \frac{\tilde{u}_i - \lambda \tilde{b}_i}{1 + 2\lambda\sigma_i}$.

We rewrite the numerator of $T_i(\lambda)$ to match the denominator:

$$T_i(\lambda) = \frac{-\frac{\tilde{b}_i}{2\sigma_i}(1 + 2\lambda\sigma_i) + \frac{\tilde{b}_i}{2\sigma_i} + \tilde{u}_i}{1 + 2\lambda\sigma_i} = -\frac{\tilde{b}_i}{2\sigma_i} + \frac{C_i}{1 + 2\lambda\sigma_i},$$

where $C_i = \frac{\tilde{b}_i}{2\sigma_i} + \tilde{u}_i$ is a constant. Let $t_i^* = -\frac{\tilde{b}_i}{2\sigma_i}$. Since the denominator $(1 + 2\lambda\sigma_i)$ grows linearly with λ , the second term decays as λ^{-1} :

$$T_i(\lambda) = t_i^* + O(\lambda^{-1}).$$

We substitute this into the quadratic Q_i . Note that t_i^* is a critical point of Q_i , satisfying $Q_i'(t_i^*) = 2\sigma_i t_i^* + \tilde{b}_i = 0$. Using the Taylor expansion around t_i^* :

$$Q_i(T_i(\lambda)) = Q_i(t_i^*) + \underbrace{Q_i'(t_i^*)}_{0} \cdot O(\lambda^{-1}) + O(\lambda^{-2}).$$

Summing these terms:

$$E(\lambda) = c_{\theta} + \sum_{i \in I_{\text{range}}} Q_i(t_i^*) + O(\lambda^{-2}) = S + O(\lambda^{-2}).$$

Since $S = 0$, the rational function decays as $O(\lambda^{-2})$. This implies that the degree of the numerator $P(\lambda)$ is exactly two less than the denominator:

$$\text{EDdegree}(\mathcal{V}_{c,c'}^{\theta}) = \deg(D) - 2 = 2r - 2.$$

□

B.10 Proof of Corollary 4.7

Corollary 4.7. *The ED degree $\text{EDdegree}(\mathcal{V}_{c,c'}^\theta)$ is exactly $2n$ if and only if all of the following hold:*

- A_θ is non-singular: $\text{rank}(A_\theta) = n$;
- $\mathcal{V}_{c,c'}^\theta$ is non-singular: $\text{rank}(M_\theta) = n + 1$;
- A_θ has distinct eigenvalues: the discriminant of the characteristic polynomial of A_θ is non-zero.

Proof. We examine the three cases from Theorem 4.6. First, consider the case when $\text{rank}(M_\theta) = \text{rank}(A_\theta) + 2$. The degree is given by $2r + 1$. Since this value is always odd, it cannot equal the even integer $2n$. Next, consider the case when $\text{rank}(M_\theta) = \text{rank}(A_\theta)$. The degree is given by $2r - 2$. Because the number of distinct eigenvalues r cannot exceed the dimension n , the maximum possible degree in this case is $2n - 2$, which is strictly less than $2n$. Therefore, the degree can equal $2n$ only in the case when $\text{rank}(M_\theta) = \text{rank}(A_\theta) + 1$. In this scenario, the degree is $2r$. Setting $2r = 2n$ implies that $r = n$. This means that the matrix A_θ must have exactly n distinct non-zero eigenvalues. Hence, A_θ has full rank with no zero or repeated eigenvalues. Conversely, if A_θ is non-singular with distinct eigenvalues and $\mathcal{V}_{c,c'}^\theta$ is non-singular, we are in the case with $r = n$, yielding the ED degree of $2n$. \square

Appendix C Experiments and Implementation Details

In this section, we provide additional details about the experiments and implementation. Following the methodology of SoundnessBench (Zhou et al., 2025), we construct a soundness benchmark for evaluating the correctness of neural network verifiers on polynomial neural networks. The key idea is to train networks with deliberately planted counterexamples: for a subset of test instances, adversarial perturbations within the ℓ_2 -ball of radius ϵ are known to exist by construction. A sound verifier must not certify these instances as robust. We additionally include “clean” instances (without planted counterexamples) to avoid the case that the verifier always returns negative (i.e., never certifies any instance), which would trivially achieve perfect soundness on the planted counterexample instances. It is worth noting that these “clean” instances are not necessarily robust.

Benchmark configurations We generate 8 benchmark configurations by taking the Cartesian product of the following variable parameters, while keeping input dimension fixed at 8 and output dimension at 2 (binary classification). The hidden dimensions are chosen from $\{6, 10\}$, the activation degrees from $\{2, 3\}$ (quadratic and cubic polynomial activations), and the perturbation radii from $\{0.2, 0.5\}$. The total number of configurations is thus $2 \times 2 \times 2 = 8$. Each configuration contains 10 unverifiable instances (with planted counterexamples) and 10 clean instances, giving 160 instances in total across the benchmark.

Data generation For each configuration, we sample n input points $x_0^{(i)} \in \mathbb{R}^d$ uniformly from $[-1, 1]^d$, and assign random binary labels $y^{(i)} \in \{0, 1\}$. For the unverifiable instances, we construct adversarial perturbations $\delta^{(i)}$ such that the perturbed point $x_{\text{cex}}^{(i)} = x_0^{(i)} + \delta^{(i)}$ lies within the ℓ_2 -ball of radius ϵ around $x_0^{(i)}$, but is assigned a different target label $y_{\text{cex}}^{(i)} \neq y^{(i)}$. The perturbation is sampled as follows:

- Sample a random direction v uniformly on the unit sphere by drawing from a standard normal distribution and normalizing: $v = z/\|z\|_2$, where $z \sim \mathcal{N}(0, I_d)$.
- Sample a magnitude m uniformly from $[r \cdot \epsilon, \epsilon]$, where $r = 0.98$.
- Set $\delta = m \cdot v$.

The parameter r controls how close to the boundary of the ℓ_2 -ball the counterexample is placed. By setting $r = 0.98$, counterexamples are placed in a thin shell near the boundary, making them harder for adversarial attacks to discover while still lying strictly within the perturbation ball. For binary classification, the target label is simply the flipped label $y_{\text{cex}} = 1 - y$. Clean instances consist of input points and labels generated identically to the unverifiable case, but without any planted counterexamples. These serve as a control group to evaluate whether the verifier produces false negatives (i.e., fails to verify instances that may in fact be robust).

Model architecture and training We use polynomial neural networks (PNNs), which replace standard nonlinear activations (e.g., ReLU) with polynomial activation functions. The network consists of linear layers interleaved with element-wise polynomial activations, except after the final output layer:

$$x \xrightarrow{W_1, b_1} h_1 \xrightarrow{\sigma} h'_1 \xrightarrow{W_2, b_2} h_2 \xrightarrow{\sigma} \dots \xrightarrow{W_L, b_L} \text{output}$$

We use homogeneous polynomial activations of degree d , i.e., $\sigma(x) = x^d$. The activation is applied element-wise across each hidden dimension. The use of polynomial activations is essential: it makes the entire network a polynomial function of its inputs, enabling exact algebraic verification via homotopy continuation. Linear layer weights and biases use PyTorch’s default initialization. Each model is trained with a dual-objective loss that simultaneously achieves correct classification on clean points and successful misclassification on planted counterexamples. The total loss combines two terms:

$$\mathcal{L} = \mathcal{L}_{\text{CE}} + \mathcal{L}_{\text{margin}}$$

Cross-entropy loss \mathcal{L}_{CE} is applied to all input points x_0 (both unverifiable and clean instances) with their correct labels, encouraging the model to classify them correctly. Margin loss $\mathcal{L}_{\text{margin}}$ is applied only to the counterexample points x_{cex} from unverifiable instances. This is a hinge-style loss that encourages the model to assign a higher logit to the target (incorrect) label than to the original (correct) label:

$$\mathcal{L}_{\text{margin}} = \frac{1}{n} \sum_{i=1}^n \max \left(0, f_{y^{(i)}}(x_{\text{cex}}^{(i)}) - f_{y_{\text{cex}}^{(i)}}(x_{\text{cex}}^{(i)}) + m \right)$$

where $f_k(x)$ denotes the logit for class k , and $m = 0.01$ is the margin.

We use the *Adam* optimizer (Kingma and Ba, 2015) with a cyclic learning rate schedule and a full batch size. The base learning rate is set to $\eta = 0.001$, and the cyclic schedule linearly ramps up during the first half of training and linearly decays during the second half:

$$\eta(t) = \begin{cases} \eta \cdot \frac{t}{T/2} & \text{if } t < T/2 \\ \eta \cdot \frac{T-t}{T/2} & \text{if } t \geq T/2 \end{cases}$$

where $T = 5,000$ is the total number of epochs.

Table 2: Evaluation of our verifier on the Soundness Benchmark for polynomial neural networks.

TRAINING SETTINGS			RESULTS		
h	d	ϵ	FALSIFIED (UNVERIFIABLE)	FALSIFIED (CLEAN)	RUNNING TIME (s)
6	2	0.2	100%	60%	0.0448 (0.0063)
6	2	0.5	100%	60%	0.0546 (0.0242)
6	3	0.2	100%	20%	5.8013 (0.5377)
6	3	0.5	100%	40%	5.4401 (0.2486)
10	2	0.2	100%	30%	0.0331 (0.0063)
10	2	0.5	100%	50%	0.0335 (0.0102)
10	3	0.2	100%	30%	4.6127 (0.1721)
10	3	0.5	100%	50%	4.4646 (0.2993)

Verification Verification is built upon *HomotopyContinuation.jl*, which computes the exact robust radius for each test point. Given an input instance (ξ, ϵ) , verification is determined by whether the model admits an adversarial example within an ℓ_2 -ball of radius ϵ around ξ . If no such adversarial example exists, the instance is classified as *verified*. Otherwise, the instance is *falsified*, indicating the presence of a valid counterexample within the allowed perturbation region.

For instances designated as *unverifiable* by construction, a sound verification method must always report falsification, since counterexamples are guaranteed to exist. Any verification claim on an unverifiable instance therefore constitutes a false positive and signals a soundness error in the verifier. In contrast, for clean instances, both verification and falsification are acceptable outcomes, depending on the true robustness of the model at the given input. This distinction allows us to separately evaluate verifier soundness on unverifiable

instances and verifier precision on clean instances. Table 2 summarizes the verification results across all 8 benchmark configurations. The verifier achieves perfect soundness on all unverifiable instances, correctly identifying all planted counterexamples. On clean instances, the verifier successfully falsifies a significant fraction, demonstrating its ability to detect non-robustness even without planted counterexamples. The average verification time per instance is also reported, showing efficient performance across configurations.